J Physiol 602.4 (2024) pp 569–596

The Journal of Physiology

The effects of daily dose of intense exercise on cardiac responses and atrial fibrillation

Renée A. Gorman[1,2], Simona Yakobov[1,2], Nazari Polidovitch[1], Ryan Debi[1], Victoria C. Sanfrancesco[2,3], David A. Hood[2,3], Robert Lakin[1,2] and Peter H. Backx[1,2]

[1]*Department of Biology, York University, Toronto, ON, Canada*
[2]*Muscle Health Research Centre, York University, Toronto, ON, Canada*
[3]*Department of Kinesiology and Health Science, York University, Toronto, ON, Canada*

Handling Editors: Bjorn Knollmann & Brian Delisle

The peer review history is available in the Supporting Information section of this article (https://doi.org/10.1113/JP285697#support-information-section).

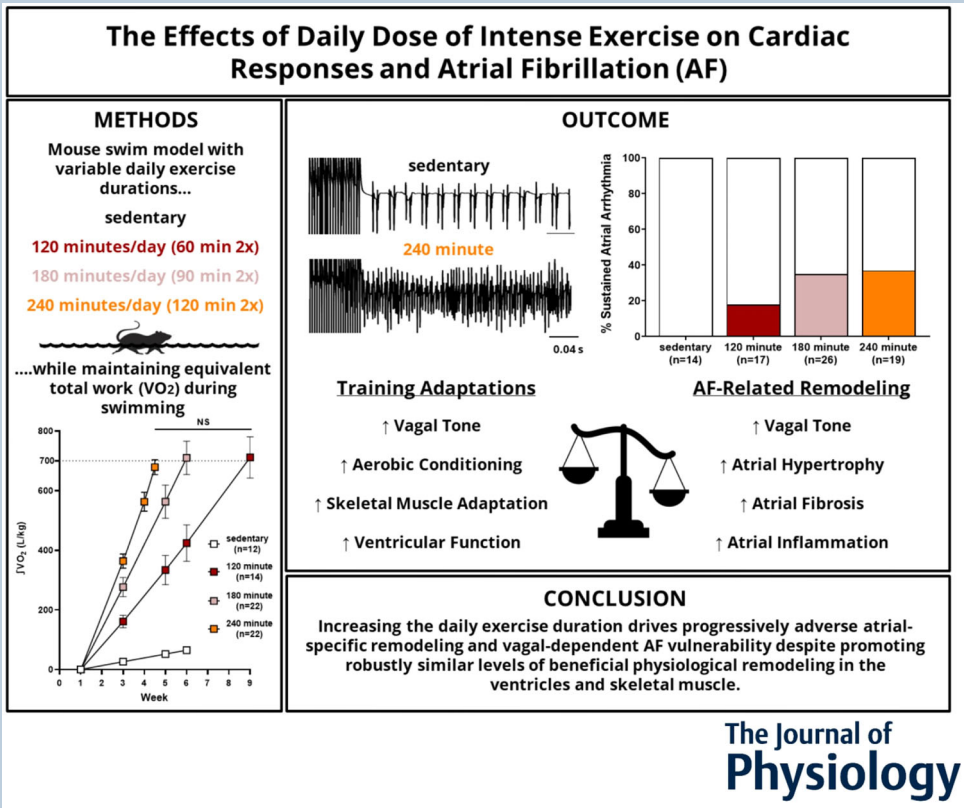

Abstract Atrial fibrillation (AF) is a supraventricular tachyarrhythmia that is strongly associated with cardiovascular (CV) disease and sedentary lifestyles. Despite the benefits of exercise on overall health, AF incidence in high-level endurance athletes rivals that of CV disease patients, suggesting a J-shaped relationship with AF. To investigate the dependence of AF vulnerability on exercise, we varied daily swim durations (120, 180 or 240 min day^{-1}) in 7-week-old male CD1 mice. We assessed mice after performing equivalent amounts of cumulative work during swimming (i.e. ∼700 L O_2 kg^{-1}), as determined from O_2 consumption rates ($\dot{V}_{O_2}$). The mean $\dot{V}_{O_2}$

R. A. Gorman and S. Yakobov contributed equally to this work and share first authorship.

DOI: 10.1113/JP285697

during exercise increased progressively throughout the training period and was indistinguishable between the swim groups. Consistent with similar improvements in aerobic conditioning induced by swimming, skeletal muscle mitochondria content increased ($P = 0.027$) indistinguishably between exercise groups. Physiological ventricular remodelling, characterized by mild hypertrophy and left ventricular dilatation, was also similar between exercised mice without evidence of ventricular arrhythmia inducibility. By contrast, prolongation of daily swim durations caused progressive and vagal-dependent heart rate reductions ($P = 0.008$), as well as increased ($P = 0.005$) AF vulnerability. As expected, vagal inhibition prolonged ($P = 0.013$) atrial refractoriness, leading to reduced AF vulnerability, although still inducible in the 180 and 240 min swim groups. Accordingly, daily swim dose progressively increased atrial hypertrophy ($P = 0.003$), fibrosis ($P < 0.001$) and macrophage accumulation ($P = 0.006$) without differentially affecting the ventricular tissue properties. Thus, increasing daily exercise duration drives progressively adverse atrial-specific remodelling and vagal-dependent AF vulnerability despite robust and beneficial aerobic conditioning and physiological remodelling of ventricles and skeletal muscle.

(Received 17 September 2023; accepted after revision 8 December 2023; first published online 3 February 2024)
Corresponding authors Peter H. Backx and Robert Lakin: Department of Biology, York University, 354 Farquharson Building, 4700 Keele Street, Toronto, Ontario M3J 1P3, Canada. Email: pbackx@yorku.ca, lakinrob@yorku.ca

Abstract figure legend A dose–response relationship exists between physical activity and cardiovascular health outcomes, wherein moderate exercise is protective, whereas intense endurance sport can increase atrial fibrillation (AF) susceptibility. We compared the cardiovascular adaptations of mice to variations in daily swimming durations (120, 180 or 240 min day^{-1}). After performing the same total work during swimming (estimated by measuring oxygen consumption during exercise), we found that increasing daily exercise doses promoted AF vulnerability, as well as atrial fibrosis, inflammation and hypertrophy, despite stimulating equivalent physiological ventricular adaptations and aerobic conditioning. Because oxygen consumption in mice during exercise matches equivalent measures in humans (i.e. MET-h week^{-1}), we argue that our findings shed light on the dose-dependency of AF vulnerability in athletes. In particular, we suggest that the atrial-specific changes observed, as the amounts of daily exercise are increased, arise from progressive elevations in filling pressures, a feature common in most AF patients.

Key points

- Previous studies have suggested that a J-shaped dose–response relationship exists between physical activity and cardiovascular health outcomes, with moderate exercise providing protection against many cardiovascular disease conditions, whereas chronic endurance exercise can promote atrial fibrillation (AF).
- We found that AF vulnerability increased alongside elevated atrial hypertrophy, fibrosis and inflammation as daily swim exercise durations in mice were prolonged (i.e. $\geq$180 min day^{-1} for 6 weeks).
- The MET-h week^{-1} (based on O_2 measurements during swimming) needed to induce increased AF vulnerability mirrored the levels linked to AF in athletes.
- These adverse atria effects associated with excessive daily exercise occurred despite improved aerobic conditioning, skeletal muscle adaptation and physiological ventricular remodelling.
- We suggest that atrial-specific changes observed with exercise arise from excessive elevations in venous filling pressures during prolonged exercise bouts, which we argue has implications for all AF patients because elevated atrial pressures occur in most cardiovascular disease conditions as well as ageing which are linked to AF.

Introduction

International guidelines recommend 150 min of moderate physical activity (PA) or 75 min of high-intensity exercise per week for optimal health outcomes (Singh et al., 2020). The benefits of regular exercise are broad, ranging from reduced metabolic disorders (Carbone et al., 2019), lower incidence of selected cancers (Rezende et al., 2018)

and improved cardiorespiratory health (Swain, 2005), even in patients with cardiovascular-related diseases (Fiuza-Luces et al., 2018). Nevertheless, some studies have concluded that high-intensity PA is associated with increased all-cause mortality risk, particularly in vulnerable populations (Mittleman et al., 1993), although these conclusions are disputed (Kontro et al., 2018). The dichotomous effects of exercise are also evident for atrial fibrillation (AF), for which the age-dependent risk for AF is higher in sedentary, obese and diabetic populations (Al-Kaisey & Kalman, 2021; Bohne et al., 2019), as well as elite endurance athletes (Mont, 2002), compared to the general population. Although the relationship between exercise and AF is complex (Buckley et al., 2020), studies have demonstrated that intensity (Gerche & Schmied, 2013), duration (Lee et al., 2014), frequency (Aizer et al., 2009) and total dose (Elosua et al., 2006) can increase AF risk by as much as 10-fold (Elliott et al., 2018). In particular, using metabolic equivalence of task (MET) measures of exercise intensity, it has been proposed that AF incidence increases when exercise exceeds 55 MET-h week^{-1} and performed at a high intensity (i.e. 12 to 15 METs) (Franklin et al., 2020). Moreover, a study in competitive cross-country skiers found that AF incidence tracked with performance and number of competitions, suggesting a cumulative effect of high-intensity exercise on AF risk (Andersen et al., 2013).

The mechanisms by which exercise mediates increased AF vulnerability are unclear, even though many features of the athlete's heart, such as atrial enlargement, reduced atrial refractoriness and enhanced vagal tone (Estes & Madias, 2017) are linked clearly to AF vulnerability (Bizhanov et al., 2023). Moreover, AF in cardiovascular (CV) disease patients are invariably associated with inflammation (Yamashita et al., 2010) and atrial fibrosis (Sohns & Marrouche, 2020), the latter of which has also been reported in rodent exercise models (Aschar-Sobbi et al., 2015; Benito et al., 2011), as well as veteran marathon athletes (Peritz et al., 2020), although controversial (Małek & Bucciarelli-Ducci, 2020). In this regard, it is important to note that intense exercise causes marked elevations in venous filling pressure (rising to 20–40 mmHg) (Reeves et al., 1990), which is also a hallmark feature of most CV disease conditions linked to AF (Vranka et al., 2007), and is recognized as a potent stimulus for hypertrophy, fibrosis and inflammation (De Jong et al., 2011).

It has been suggested that the relationship between exercise 'dose' and AF risk is J-shaped, such that light to moderate exercise reduces AF risk, whereas excessive exercise promotes AF (Buckley et al., 2020). However, such conclusions are based on studies that relied on self-reporting for the quantification of exercise (Gerche & Schmied, 2013). To better understand this relationship, we quantified the exercise effort (work) of mice swimming for either 120, 180 or 240 min day^{-1} (split into two sessions) by measuring O_2 consumption rates and compared the cardiac and skeletal muscle responses after all mice had achieved the same total work during training (~700 L O_2 kg^{-1}). We observed that aerobic conditioning (i.e. mean $\dot{V}_{O_2}$ during swimming) increased with time spent exercising, regardless of the daily swim dose. Nevertheless, prolonging daily swim durations caused progressive vagal-dependent decreases in heart rate (HR) and increases in AF vulnerability, as well as atrial hypertrophy, fibrosis and immune cell (macrophage) infiltration without impacting physiological remodelling in the ventricles and skeletal muscle or promoting ventricular arrhythmia vulnerability.

Methods

Ethical approval

Male CD1 mice were purchased at 7-weeks of age from Charles River (Wilmington, MA, USA), housed in identical environments (12:12 h light/dark photocycle) and consumed the same *ad libitum* diets. After acclimatizing for 1 week, mice were assigned randomly into four groups: sedentary controls or one of three swim groups. All procedures performed on the mice were approved by the Animal Care Committee at York University (2019-15). All experimental procedures conformed to the Canadian Council on Animal Care standards that meet the ethical principles under which

Renée A. Gorman graduated with an MSc at York University in August 2023. She joined the Backx laboratory initially for her Master's project and is currently a first-year PhD candidate where she continues her passion for studying cardiac electrophysiology. Her research focuses primarily on the ventricular conduction system, including its associated ion channels and their spatial and temporal organization across various species by combining electrophysiological and microscopy techniques. **Simona Yakobov** obtained her MSc with the Backx group in September 2020 and subsequently joined as a laboratory technician for the year following. She then pursued an industry career focusing on project management in the field of drug development. Currently, Simona works as an Alliances Manager at Menten AI, a biotechnology start-up building a generative AI platform for peptide therapeutics. She focuses on building strategic partnerships within the biopharmaceutical industry using her interdisciplinary expertise in drug development, scientific discovery and project management.

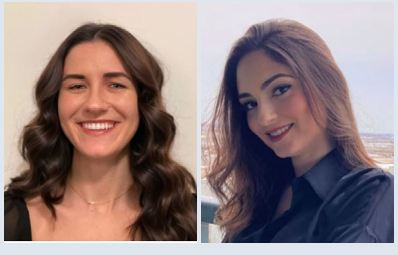

The Journal of Physiology operates and comply with their animal ethics checklist (Grundy, 2015).

Swim training protocol and O_2 measurements

Swim training took place in tanks (3.1 gallons, 30 cm in diameter, 16.5 cm water depth) filled with thermoneutral water (30–32°C)(Speakman, 2013) and equipped with submersible pumps that generate circular currents. To quantify work and effort associated with daily exercise, we measured O_2 consumption rates (i.e. $\dot{V}_{O_2}$) during swimming, as described further below. Because CD1 mice intrinsically swim against water currents (see Supporting information, Video S1), we initially attempted to vary exercise dose by systematically altering flow rates from 10 to 20 L min^{-1} in the swim tanks. Unfortunately, our $\dot{V}_{O_2}$ measurements revealed no differences in the rates of O_2 consumption during swimming (i.e. exercise effort) when water flow rates were varied (Fig. 1), even after mice had undergone swim training for 6 weeks. The absence of differences in $\dot{V}_{O_2}$ as a function of water flow rate suggests that mice are able to self-regulate their exercise intensity. This possibility is supported by the observation that, after swimming for ∼15 min, mice move routinely and intermittently toward the centre of the tank where the current is weaker. This self-regulation behaviour is also reflected in the typical representative $\dot{V}_{O_2}$ recordings (discussed in detail later), showing that the mean $\dot{V}_{O_2}$ magnitudes rise quickly and peak in the first 15 min of each swim and decline thereafter to a slower steady rate, possibly reflecting an onset of fatigue or reduced exercise effort.

Because varying exercise intensity was not possible, we elected to investigate the effects of exercise dose on cardiac responses by altering the daily durations of the swims. Since we showed previously that swimming mice for 90 min twice daily resulted in adverse atrial remodelling and AF vulnerability (Aschar-Sobbi et al., 2015), we swam mice for either 120, 180 or 240 min day^{-1} (divided into two swims between 09.30 h and 11:30 h and between 14.30 h and 17.30 h), separated by a 4 h rest period. Before mice began training, each group was acclimatized to the apparatus by completing an initial 30 min swim session that increased by 10 min each day and progressed variably until reaching the target duration (Table 1). After acclimatization, mice swam for a varying number of weeks so that each mouse achieved the same cumulative dose of exercise, as determined by the total O_2 consumed (i.e. ∼700 L O_2 kg^{-1}) during swimming. All groups were sampled during weeks 1 and 3 of swim training. O_2 consumption was also measured in the 240 min group at week 4, in the 180 min group at weeks 5 and 6, and in the 120 min group at week 5, 6 and 9. As a result, mice exercising for 120 min each day swam for 9 weeks (i.e. ∼90 swims) on average, whereas the 180 min mice

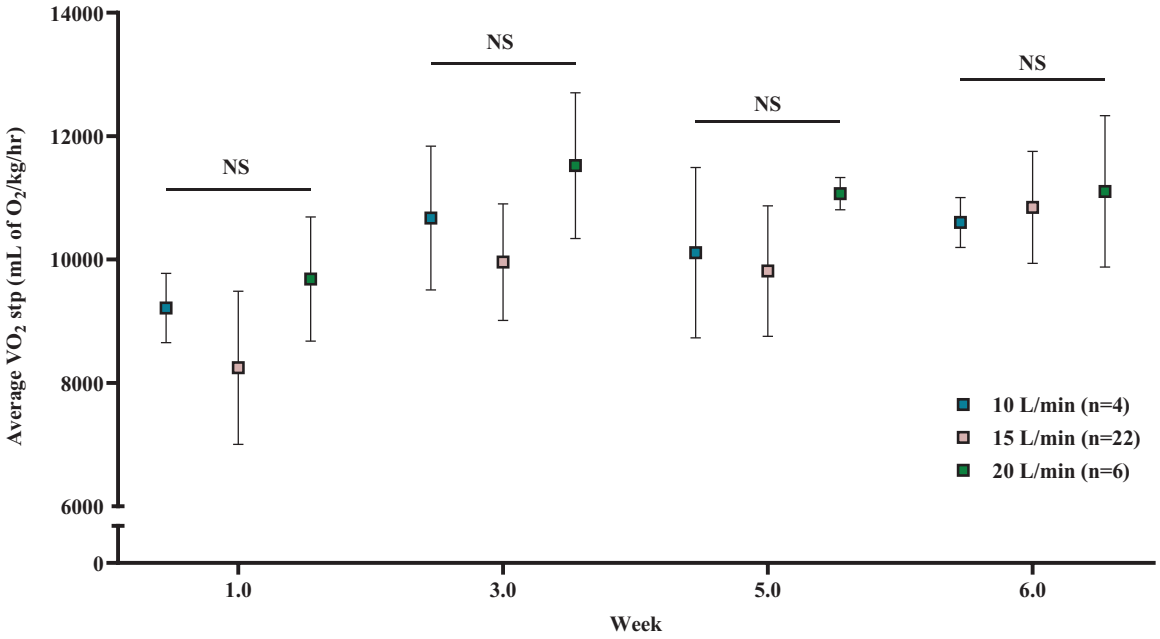

Figure 1. Self regulation behaviour of mice during swimming
Pairs of mice were placed in a swim apparatus and O_2 consumption ($\dot{V}_{O_2}$) was measured using a modified calorimetry system. Swimming behaviour was monitored and mice swam against a water current provided by a submerged pump. All groups swam for 180 min against water currents of 10, 15 or 20 L min^{-1}. Averaged $\dot{V}_{O_2}$ measurements recorded during swimming revealed no differences when mice swam against different water currents. The *n* values indicate the number of mice examined in each group. Data are the mean ± SD. *$P < 0.05$ using ANOVA with Tukey's multiple comparisons tests. [Colour figure can be viewed at wileyonlinelibrary.com]

Table 1. Overview of acclimation period for the swim duration protocols

	120 min day^{-1}						
	Monday	Tuesday	Wednesday	Thursday	Friday	Saturday (rest)	Sunday (rest)
Week 1	30 min	40 min	50 min	60 min			
	180 min day^{-1}						
	Monday	Tuesday	Wednesday	Thursday	Friday	Saturday (rest)	Sunday (rest)
Week 1	30 min	40 min	50 min	60 min	70 min		
Week 2	80 min	90 min					
	240 min day^{-1}						
	Monday	Tuesday	Wednesday	Thursday	Friday	Saturday (rest)	Sunday (rest)
Week 1	30 min	40 min	50 min	60 min	70 min		
Week 2	80 min 90 min	100 min 110 min	120 min				

The swim acclimation schedules for the three groups are shown. After acclimatization, mice swam twice daily between 09.30 h and 11.30 h and between 14.30 h and 17.30 h (separated by 4 h) following their respective training protocols until the required termination point was reached based on the total O_2 consumption during exercise. Sedentary mice were placed into the water for 10 min and without currents.

swam for 6 weeks (∼60 swims) and 240 min mice swam for four and a half weeks (∼45 swims) (sample traces are shown in Fig. 3). Sedentary control mice were also placed in water containers without current for 10 min twice daily for 6 weeks.

The rate of O_2 consumption by mice was calculated from the difference between the dried $\%O_2$ of the inflow and outflow air using the measured atmospheric pressure and based on the assumption that changes in O_2 throughout the swim were exclusively caused by mouse consumption in response to exercising. This was accomplished with a custom-built system that measured $\%O_2$, temperature, humidity and pressure of the air, flowing at a rate of 4 L min^{-1} into and 1 L min^{-1} out of the sealed swim chambers (Oxymax; Columbus Instruments, Columbus, OH, USA; BME280; Adafruit Industries, New York, NY, USA). The $\%O_2$ was calibrated using dried room air (at 20.95% O_2) and a gas mixture of 20.5% O_2 plus 5000 ppm CO_2, balanced with N_2 (Praxair, Inc., Danbury, CT, USA). Because the Oxymax sensor measures electrochemically the partial pressure of O_2, it is necessary to correct for changes in atmospheric pressure, which was continuously monitored. Additionally, the Oxymax sensors suffer from baseline drifting with time. To correct baseline drift, O_2 measurements were adjusted as needed by recording atmospheric $\%O_2$ (20.95%) for 10 mins before and for 10 mins after the swims. Thus, we estimated the $\dot{V}_{O_2}$ using the equation:

$$\dot{V}_{O_2} = \left(\frac{20.95\%}{100} - \frac{\%O_{2(\text{outflow})}}{100}\right) * \frac{P_{atm} - P_{H2O\,in}}{RT_{in}} * F$$

where $\%O_{2\,(\text{outflow})}$ is the calibrated, pressure compensated and baseline corrected estimates of the $\%O_2$, F is the flow rate of atmospheric air into the system and P_{H2O} is the partial pressure of water estimated using the Magnus equation. The V_{O2} values were then divided by the weight of the mouse and converted to standard pressure (101.325 kPa) and temperature (273.15 K) to establish subsequently that each group consumed 700 L O_2 kg^{-1} during swimming by the end of the training period.

Echocardiography

Left ventricular echocardiographic assessments were made in anaesthetized mice. Anaesthesia was induced by placing mice in a chamber with 3% isoflurane–oxygen mixture. Thereafter, mice were placed in the supine position on a heating pad and anaesthesia was maintained via an inhalation mask with an ∼1.5% isoflurane–oxygen mixture, as described previously (Lakin et al., 2018). Core temperature was monitored continuously with a rectal probe (THM 150; Indus Instruments, Webster, TX USA) and maintained between 36.9 and 37.3°C. Respiratory rates were maintained from 90 to 120 breaths min^{-1} by slightly adjusting the percentage of isoflurane, as needed. Electrocardiograms were recorded in the lead II configuration. Chest hair was removed (Nair; Church and Dwight, Princeton, NJ, USA) and an acoustic coupling gel was applied (Aquasonic 100; Parker Laboratories Inc., Fairfield, NJ, USA). Left ventricular structural and functional indices (including end-diastolic diameter, end-systolic diameter, posterior wall thickness, ejection

fraction and fractional shortening) were assessed using a 30 MHz ultrasonic linear transducer (Vevo 2100; VisualSonics Inc., Toronto, ON, Canada) in the transthoracic B-mode and M-mode recording configurations.

Surface electrocardiography (ECG) with pharmacological blockade

ECG assessments were made in mice that were anaesthetized precisely as described for the ultrasound recordings. Surface ECGs (sECGs) were achieved by inserting subdermal platinum electrodes (F-E7; Grass Technologies, West Warwick, RI, USA) that were connected to high impedance amplifiers (Gould ACQ-7700; Data Sciences International, New Brighton, MN, USA). Recordings were collected and analyzed with the Ponemah Physiology Platform (P3) software (Data Sciences International). Recordings were marked for R–R intervals to estimate HRs using P3 Plus (Data Sciences International). All measurements were made after a 20 min stabilization window. Thereafter, baseline sECG recordings were averaged over 5 min to determine resting HR. We also examined the effects of cardiac autonomic nerve blockers as follows. First, atropine sulphate (2 mg kg^{-1} body weight) was injected I.P. to block cardiac parasympathetic nerve activity. After a 20 min stabilization period, HRs were again estimated by averaging over 5 min. Next, propranolol hydrochloride (10 mg kg^{-1} body weight) was injected I.P. to inhibit cardiac sympathetic nerve activity and HR was estimated 20 min later by averaging over a 5 min interval. Note that, after administration of both atropine and propranolol, we expect that mice have complete autonomic blockade because the half-time of atropine is 2–4 h (McEvoy, 2012).

Cardiac contractility assessments using invasive haemodynamics

Haemodynamic assessments were made in mice that were anaesthetized as described above for the echocardiographic measurements. The right common carotid was then dissected by creating a midline incision below the chin, gently moving aside the salivary glands, locating the pulsating vessel parallel to the trachea and carefully separating the connective tissue that attaches the carotid artery to the white vagus nerve. Subsequently, an anterior suture was tied around the vessel with two additional threads added posteriorly; one acted as a bridge to prevent blood loss and the other was tied around the artery after creating a ventral incision and inserting the 1-Fr pressure-transducing catheter (Scisense, London, ON, Canada) that was advanced from the proximal aorta into the left ventricle. Data were then acquired at 5000 Hz using the Scisense ADV500 control unit (Scisense, London, ON, Canada) with Acqknowledge acquisition software (Biopic, Goleta, CA, USA). A minimum equilibration period of 15 min preceded 5 min of baseline data acquisition. Inotropic reserves were then determined following I.P. injection of dobutamine (100 μL, 1.5 mg kg^{-1}). Given the dobutamine half-life (2 min), there were 20 min between the administration and subsequent steady-state measurements for drug washout.

In vivo effective refractory period and AF inducibility measurements

Cardiac electrical remodelling and arrhythmia vulnerability were assessed as previously described (Aschar-Sobbi et al., 2015). Briefly, the mice were anaesthetized as described in the echocardiographic measurements. The right jugular vein, which usually sits at a 45° angle with the frontal and longitudinal axes, was exposed by making a superficial incision at the skin surface and pulling away muscle and connective tissue. A suture was then placed around the anterior end of the exposed jugular vein. Next, a small incision was made into the jugular, posterior to the suture, to allow a 2-Fr octopolar recording/stimulating catheter (CI'BER Mouse; NuMed, Hopkinton, NY, USA) to be inserted into the vessel. After applying a second suture around the catheter posterior to the incision, the catheter was guided into the right atrium then right ventricle via the superior vena cava. The correct placement of the catheter required that the electrical signal recorded between electrodes 3 and 4 (of the octapolar catheter) show a prominent His bundle depolarization signal. The arrangement of the catheter within the heart following insertion is illustrated in Fig. 2.

A 15 min stabilization period preceded all electrophysiological assessments. Timed bipolar electrical stimulations were applied (via adjacent electrodes in the octapolar catheter) to selected regions of the heart (i.e. atria or ventricles) using an electrical stimulator with cycle control (Pulsar 6i; Frederick Haer Co, Bowdoin, ME, USA). Intracardiac electrical signals (i.e. electrograms) from selected pairs of adjacent electrodes of the octapolar catheter (i.e. bipolar signals), as well as a pair of subdermal needles for lead II surface ECGs, were amplified and recorded (Gould ACQ-7700; Data Sciences International). Electrograms were analyzed with P3 acquisition software (Data Sciences International).

For electric stimulation of atria or ventricles, the threshold voltage needed for electrical entrainment was determined by applying electrical pulses between adjacent electrodes of the octapolar catheter at intervals that were 20 ms below the R–R interval; the applied voltage was increased progressively until the heart was electrically entrained (i.e. QRS complexes were observed with each applied pulse). All pulsing protocols used to induce AF or

determine refractoriness (see below) were performed with stimulation voltages that were 1.5 times the threshold.

The atrial effective refractory periods (AERP), the shortest interval required before a new stimulus can elicit a subsequent action potential, were obtained using field stimulation through catheter leads 78 or 56. A series of nine premature pulses (called S1) were delivered and followed by a single (extra) stimulation (called S2) that was applied after varied times, initially being delivered below capture (∼15 ms) and increased by 5 ms increments until atrial capture (i.e. QRS complexes were generated). Upon capture, the coupling interval was reduced by 1–2 ms until QRS entrainment was lost. Two sequential assessments were used to determine the mean AERP for each mouse.

To assess atrial arrhythmia inducibility, a series of rapid programmed stimulation protocols were delivered to the high atrium (lead 78) followed by the same protocol applied to the mid atrium (lead 56). The protocols consisted of: (i) 27 pulses (of 1 ms in duration) at a 40 ms interval, reduced to 20 ms by 2 ms decrements, repeated three times, and (ii) 20 pulses (of 1 ms in duration) at a 20 ms coupling interval repeated 20 times separated by 1.5 s, followed by a 5 min break and repeated to a maximum of three times. Ventricular arrhythmia inducibility followed identical electrical protocols but was applied to lead 12. Sustained arrhythmias were reproducible episodes of rapid, chaotic and continuous atrial or ventricular activity >10 s.

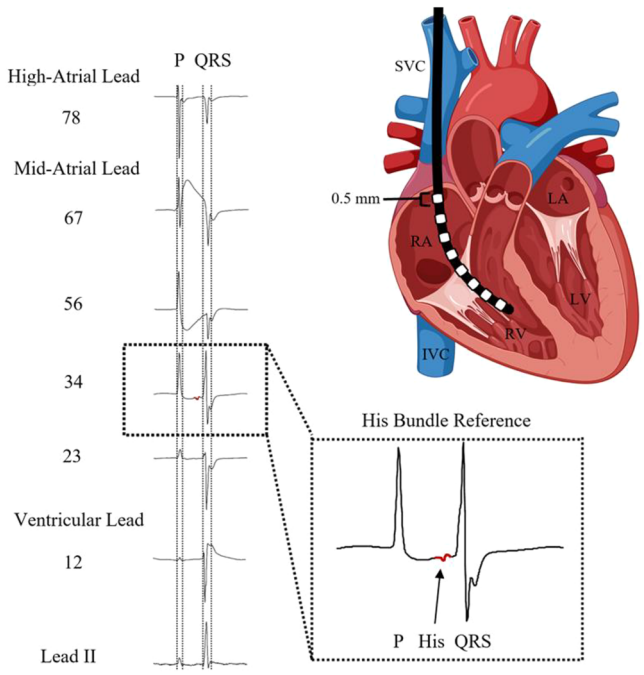

Figure 2. Intracardiac 2-Fr electrophysiology catheter placement in the right heart
The 2-Fr EP catheter (CI'BER Mouse) was introduced through the right jugular vein, directed through the right atrium and positioned within the right ventricle. The ventricular signal (QRS complex) progressively decreases from the distal (12) to proximal (78) leads, whereas the atrial signal (P wave) progressively increases. Leads 78 and 56 were used to stimulate the high and mid right atrium, whereas lead 12 was used to stimulate the right ventricle. Correct positioning was confirmed through observation of the His bundle in lead 34 as shown on the right. Lead II represents a simultaneous surface ECG recording. The eight catheter leads are 0.5 mm in length and separated by 0.5 mm between each platinum ring. LA, left atrium; RA, right atrium; LV, left ventricle; RV, right ventricle; SVC, superior vena cava; IVC, inferior vena cava. Adapted from Aschar-Sobbi et al. (2015) and created using BioRender. [Colour figure can be viewed at wileyonlinelibrary.com]

Heart tissue morphometry

After measuring body weights, mice were anaesthetized in a chamber with 3% isoflurane–oxygen mixture. Once unconscious, mice were removed and injected I.P. with 0.2–0.25 mL of heparin (1000 IU mL^{-1}; Leo Pharma, Thornhill, ON, Canada) to prevent blood clots and returned to their cage. Five minutes later, the mice were again anaesthetized in a chamber with 3% isoflurane–oxygen mixture. Subsequently, mice were placed onto a surgical pad in the supine position and anaesthesia was maintained with a 3% isoflurane–oxygen mixture delivered via an inhalation mask. The thorax was opened via a midsternal incision extending from the abdomen to the anterior of the sternum. After making an incision through the pericardium, the heart was removed rapidly. This procedure caused death by bilateral pneumothorax when the mice were still fully anaesthetized. The atria were then separated from the ventricles via an incision along the atrioventricular connective tissue, blotted with precision Kimtech wipes to remove excess fluid and subsequently weighed. The right hindlimb was also excised and stored in bleach to expose the tibia bone. Tibia lengths were determined using a calliper.

Tissue preparation for histology and immunohistological staining

Mice were anaesthetized and surgerized precisely as described above in the section on Heart Tissue Morphometry. After gaining access to the thoracic cavity, the inferior vena cava was snipped and the heart was arrested by injecting ∼5 mL of 1% KCl [in 0.01 M phosphate-buffered saline (PBS)] into the heart's apex via a 30-G needle. This was followed by injection of 20 mL of 4% paraformaldehyde (PFA) in 0.01 M PBS. This procedure caused death by bilateral pneumothorax when still fully anaesthetized. The excised hearts were placed in 35 mL of 4% PFA in 0.01 M PBS overnight. Thereafter, hearts were washed three times for 1 h with PBS, cleaned and sagittally cut with a scalpel to reveal the four-chamber

view. Individual halves underwent sequential washes with increasing concentrations of ethanol (70%, 80%, 95% and 100% × 2) and xylene (xylene–ethanol, xylene × 2) and were placed in paraffin at 60–70°C overnight for embedding in paraffin blocks the next morning. These blocks were delivered to the Centre of Phenogenomics (Toronto, ON, Canada) where tissues were sliced into 5 μm thin sections using a microtome, at three levels (100 μm apart).

Histology and immunohistological staining

For histological assessments, deparaffinization involved a series of 5 min xylene washes (xylene × 2, xylene–ethanol), 5 min ethanol washes (100% × 2, 95%, 70% and 50%) and 10 min of tap water. To quantify the cardiac collagen content of our atria and ventricles, we performed staining using picrosirius red for 1 h. Slides were rinsed in 0.5% acetic acid solution twice, dehydrated using a series of ethanol washes (95% × 2 and 100% × 2), underwent xylene washes (× 3) and were mounted with coverslips using toluene (Fisher Scientific, Waltham, MA, USA). Brightfield laser scanning microscopy imaged the picrosirius red-stained tissue at the Advanced Optical Microscopy Facility (Toronto, ON, Canada) using Aperio AT2 (Leica Biosystems, Wetzlar, Germany). Data were then analyzed using ImageJ (NIH, Bethesda, MD, USA) with the threshold method (Hadi et al., 2011), which exploits the brightness of collagen-stained tissue relative to background tissue, expressed as percentages relative to total tissue pixel counts. The analysis included the left atrial appendage, with interstitial and peri-capsular collagen examined separately, and similar-sized sections of the left ventricular free wall for total collagen content.

For immunohistological staining, mouse cardiac macrophages were identified using a rat anti-mouse primary F4-80 antibody (dilution 1:100; RRID: AB_323 806; Bio-Rad, Mississauga, ON, Canada) with secondary goat anti-rat 647 antibodies (dilution 1:100; RRID: AB_141 778; Invitrogen, Burlington, ON, Canada), both of which being previously validated in murine cardiac tissue (Mai et al., 2024; Tamaki et al., 2013). Slides were deparaffinized using three xylenes washes for 5 min each and rehydrated using a series of increasing ethanol concentrations (100% for 10 min × 2, then 95%, 70% and 50% for 5 min each). After rinsing with tap water for 10 min, heat-mediated antigen retrieval involved slides submerged in 10 mM Na-citrate buffer with 0.05% Tween 20 at pH 6.0 in a boiling pressure cooker. After pot pressurization, we counted 3 min and then indirectly washed the slides with tap water for 10 min. Three washes were then completed for 5 min each, using a wash buffer of 1000 mL of TBS (2.42 g of Tris base, 8 g of NaCl, 70 mL of ddH_2O) with 250 μL of Triton X-100 at pH 7.6. Subsequently, we used a hydrophobic barrier pen to circle the three tissue slices per slide and incubated for 1.5 h with blocking buffer (1% bovine serum albumin with 0.3 M glycine in TBS) to prevent non-specific binding. Three rinses using washing buffer at 5 min each followed, and sections were incubated in a primary antibody cocktail consisting of 1:100 primary antibody dilution in TBS with 1% bovine serum albumin and 0.025% Triton X-100 overnight at 4°C. With the three tissue slices, we incubated two with primary antibody and the other with blocking buffer to act as the negative control. Twelve hours later, slides were rinsed three times for 5 min with wash buffer and incubated with 1:100 secondary antibody dilution containing wheat germ agglutin (WGA) (staining the membrane) for 1 h at room temperature. After three additional washes for 5 min each with wash buffer, slides were mounted with anti-fade 4′,6-diamidino-2-phenylindole (DAPI)-containing medium (Invitrogen) to stain cell nuclei. Confocal laser microscopy imaged the F4-80, WGA and DAPI stained tissue at the Advanced Optical Microscopy Facility (Toronto, ON, Canada) using a AxioScan fluorescence scanner (Zeiss, Oberkochen, Germany). We counted total stained cells in the left atrial appendage and left ventricular free wall, where only cells co-staining for DAPI and F4-80 were considered true macrophages. Moreover, we normalized macrophage counts to tissue area (mm^2).

Cytochrome *c* oxidase activity

To assess mitochondrial content in skeletal muscle, we measured cytochrome *c* oxidase (COX) by diluting 15–30 mg of the tibialis anterior and gastrocnemius muscles 40-fold in an extraction buffer containing 100 mM Na-K-phosphate, 2 mM EDTA (pH 7.2) on ice. These muscles were collected from mice used for heart tissue morphometry, as described above. Tissues were then homogenized using a TissueLyser II (Qiagen, Hilden, Germany) at 30 Hz. Homogenates were sonicated three times for 3 s to disrupt cell membranes and release intact mitochondria. A test solution containing 20 mg of horse heart cytochrome *c* (C2506; MiliporeSigma, Burlingotn, MA, USA) was subsequently prepared and incubated at 30°C for 15 min to induce maximal enzymatic activity. In a 96-well plate, we added 50 μL of the tissue homogenates accordingly and dispensed 240 μL of the test solution into each well in the Citation 5 Instrument plate reader (Bio-Tek, Winooski, VT, USA). The maximal oxidation rate of cytochrome *c* was then spectrophotometrically assessed by examining 550 nm absorbance change at 30°C.

The COX activity measurement for each is an average of eight trials.

Statistical analysis

Summary data are presented as the mean ± SD unless otherwise stated. Statistical assessments primarily included the unpaired Student's *t* test, one-way analysis of variance (ANOVA) with Tukey's multiple comparisons and linear regression analysis. The results of linear regression are only included if $R^2 > 0.5$ or when comparisons were made between atrial and ventricular adverse remodelling or atrial interstitial and pericapsular fibrosis. Exceptions to the statistical assessments above include a Fisher's exact test for atrial arrhythmia data and paired *t* tests for pre- and post-pharmacological treatment. $P < 0.05$ was considered statistically significant, with analyses performed using Prism (GraphPad Software Inc., San Diego, CA, USA) or Excel (Microsoft Corp., Redmond, WA, USA).

Results

Quantification of exercise dose using O_2 consumption measurements

To assess the impact of exercise dose on cardiac remodelling, we initially attempted to vary exercise intensity by altering the flow rates of water (10–20 L min^{-1}) which were generated by pumps submerged into swim tanks. Unfortunately, although CD1 mice swim intrinsically against water currents, their $\dot{V}_{O_2}$ did not change when flow rates were varied as summarized in Fig. 1, with further details provided in the Methods. Thus, we elected to vary the exercise dose by altering daily swim durations (i.e. 120, 180 or 240 min day^{-1}, divided into two sessions, separated by 4 h) at fixed water currents (15 L min^{-1}). The number of swim sessions was adjusted for each group so that every mouse performed about the same amount of cumulative work during swimming (i.e. ∼700 L O_2 kg^{-1}), which was estimated by integrating the $\dot{V}_{O_2}$. As summarized in Fig. 3*A*, equivalent O_2 consumption between the swim groups was achieved after mice swimming for 120, 180 and 240 min day^{-1} swam for 9, 6 and 4.5 weeks, respectively (i.e. after ∼90, 60 and 45 swim sessions). Interestingly, the representative recordings shown in Fig. 3*B* reveal that $\dot{V}_{O_2}$ is 20–25% higher in the final week of swimming compared to the first week, for all three swim groups, whereas no such changes in $\dot{V}_{O_2}$ occurred for sedentary mice, who were placed in swim tanks for 10 min per session with no water current. This feature of $\dot{V}_{O_2}$ recordings is summarized in Fig. 3*C*, which shows progressive increases in mean $\dot{V}_{O_2}$ with each week of training relative to the controls. Thus, aerobic conditioning improves progressively in all three training protocols. Note also that the mean $\dot{V}_{O_2}$ during swimming reaches the same levels ($P = 0.667$) for all three groups by the end of each training protocol, demonstrating that the rate of conditioning depends directly on the number of hours spent swimming, regardless of the daily duration.

To examine whether improved aerobic conditioning with swim training was associated with altered mitochondrial content in skeletal muscle, as expected from previous studies (Amann & Calbet, 2008), we measured COX enzyme activity (per milligram of homogenates) in the tibialis anterior (TA) and gastrocnemius (GASTROC) muscles. Although one-way ANOVA comparisons found no differences (TA, $P = 0.224$ and GASTROC, $P = 0.178$) between the groups (Fig. 4*A* and *C*), when the results from the different exercise groups were pooled, we observed increased (TA, $P = 0.047$ and GASTROC, $P = 0.027$) COX activity in both skeletal muscles compared to controls (Fig. 4*B* and *D*), consistent with expected improvements in exercise capacity seen with endurance training (Holloszy & Coyle, 1984). The absence of COX activity differences between the exercised groups also aligns with the similar mean $\dot{V}_{O_2}$ levels in the three swim groups at the end of the training period, suggesting the increased COX activity does not depend on daily exercise dose but rather on the effects of cumulative training.

Cardiac adaptations in swim-trained mice as a function of exercise dose

Consistent with previous studies (Goldsmith et al., 2000), surface ECG measurements in anaesthetized mice (Fig. 5*A*) revealed that HRs were reduced ($P = 0.008$, one-way ANOVA) in all swim-trained groups compared to the non-exercised controls (Fig. 5*B*). Interestingly, linear regression analyses further revealed progressive reductions in HR ($R^2 = 0.770$, $F_{1,28} = 93.62$, $P < 0.001$) as daily exercise duration was increased (Fig. 5*C*), which correlated with one-way ANOVA comparisons in Fig. 5*B* showing that HRs were lower in the 180 min ($P = 0.007$) and 240 min ($P = 0.001$) groups compared to the 120 min mice at the end of the training period. Because changes in cardiac autonomic regulation are linked strongly to sinus bradycardia in endurance athletes (Gourine & Ackland, 2019), we examined the effects of cardiac parasympathetic and sympathetic autonomic nerve blockade on HR using atropine (2 mg kg^{-1}) and propranolol (10 mg kg^{-1}), respectively. Atropine treatment caused HR increases ($P < 0.001$, paired *t* tests) within each group and atropine's effects were more pronounced in the 180 and 240 min groups relative to either the 120 min mice ($P = 0.002$ and $P = 0.019$) or controls ($P = 0.001$

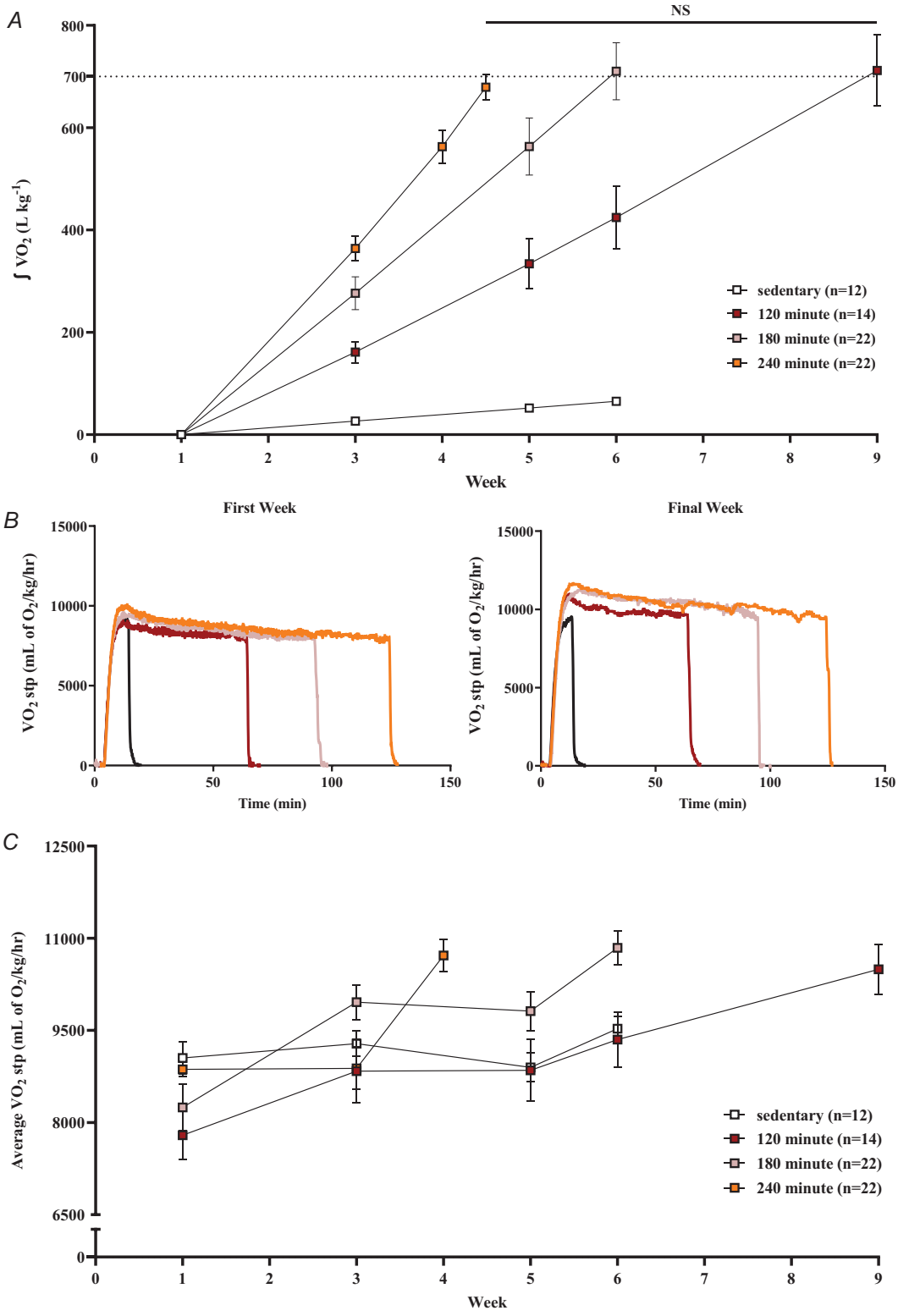

Figure 3. Characterization of changes in swim oxygen consumption with daily exercise dose
Pairs of mice swam against water currents in the swimming apparatus. Exercise behaviour was monitored and O_2 consumption ($\dot{V}_{O_2}$) was measured using a modified calorimetry system. *A*, titration analysis was performed to ensure each exercise group completed the same cumulative dose. The training terminated when mice consumed ~700 L O_2 kg^{-1} when swimming (i.e. the dotted line). *B*, representative $\dot{V}_{O_2}$ tracings from the first and final week of each swimming regime. *C*, average $\dot{V}_{O_2}$ for each swim group throughout training. The *n* values indicate the

number of mice included. Data are the mean ± SD. *P < 0.05 using a one-way ANOVA with Tukey's multiple comparisons tests. [Colour figure can be viewed at wileyonlinelibrary.com]

and P = 0.008) using one-way ANOVA comparisons (Fig. 5*D*). Thus, cardiac parasympathetic activity shows a clear dose-dependent increase as daily exercise duration is prolonged. However, the HRs after atropine treatment remained lower (P = 0.013, one-way ANOVA) for all swim groups compared to sedentary controls, with relatively small differences between the exercised groups (Fig. 5*E*). The lower HRs in the atropine-treated exercised mice compared to sedentary mice appeared to be related to differences in cardiac sympathetic regulation because after propranolol administration, in the continued presence of atropine (i.e. after complete autonomic blockade), HRs were reduced (P < 0.001, paired t tests) within each swim group, with the reductions (i.e. the propranolol-sensitive HR change) being most pronounced (P = 0.025, one-way ANOVA) in the sedentary mice compared to exercised mice, without differences between the swim groups (Fig. 5*F*). Moreover, after complete autonomic blockade no HR differences (P = 0.436, one-way ANOVA) were seen between the groups (Fig. 5*G*). These results suggest that the HR changes induced by swim exercise in our mice are not related to intrinsic SAN alterations, as seen in another mouse study (D'Souza et al., 2014), and support the conclusion that exercise reduces baseline cardiac sympathetic activity, independent of daily exercise duration.

In addition to affecting HR, exercise also increased (P = 0.002 and P = 0.040) the normalized ventricular weights (i.e. the ratio of ventricle weight to either body weight, VW/BW, or tibia length, VW/TL) relative to sedentary mice when swim data was pooled (Table 2). This exercised-induced ventricular hypertrophy was small,

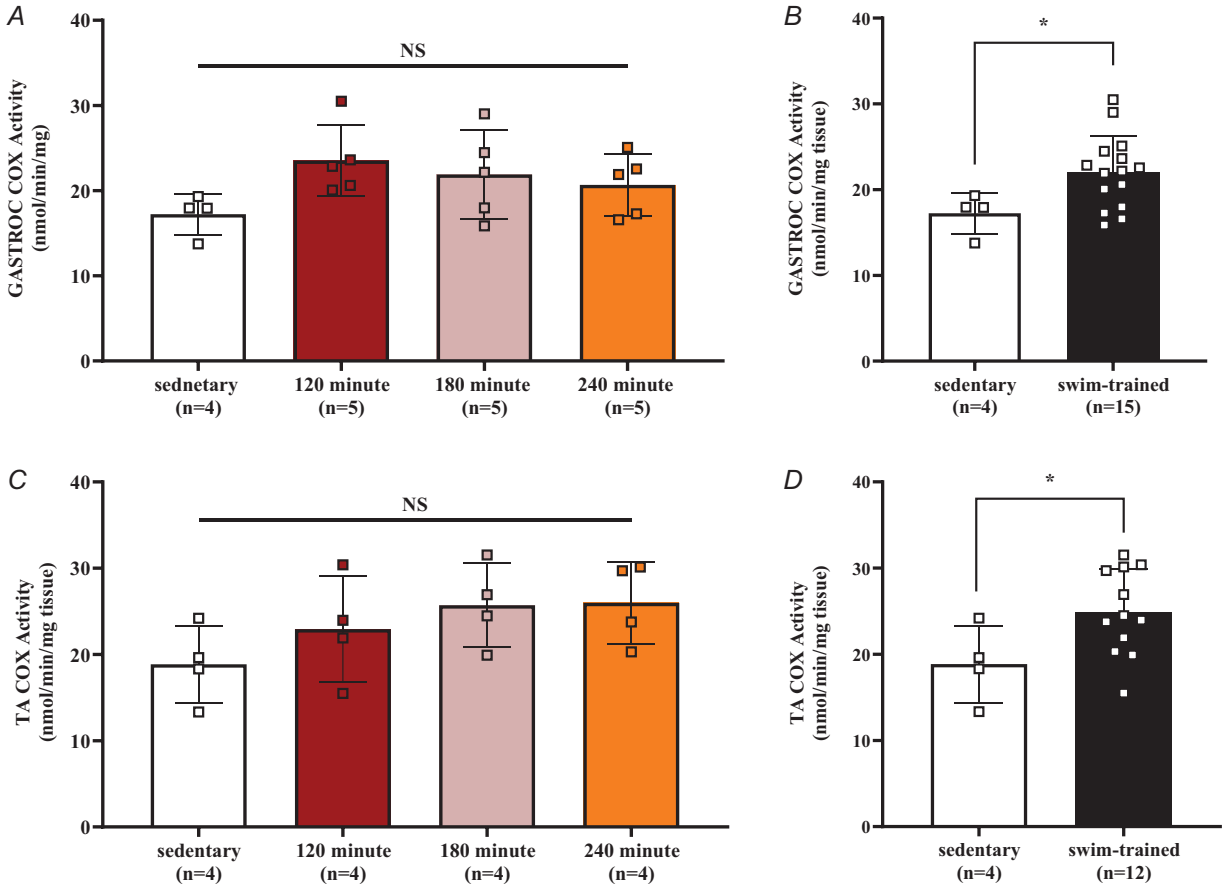

Figure 4. Skeletal muscle mitochondrial adaptation to exercise training
Following swim training termination, skeletal muscle mitochondrial content was assessed using cytochrome *c* oxidase (COX) activity in the gastrocnemius (GASTROC) (*A* and *B*) and tibialis anterior (TA) (*C* and *D*), demonstrating significant elevations when swim-trained mice were pooled, yet no differences between swim groups or when sedentary mice were compared to individual swim groups. The *n* values indicate the number of mice included. Data presented as the mean ± SD. *P < 0.05 using one-way ANOVA with Tukey's multiple comparisons tests (*A* and *C*) or unpaired Student's t tests (*B* and *D*). [Colour figure can be viewed at wileyonlinelibrary.com]

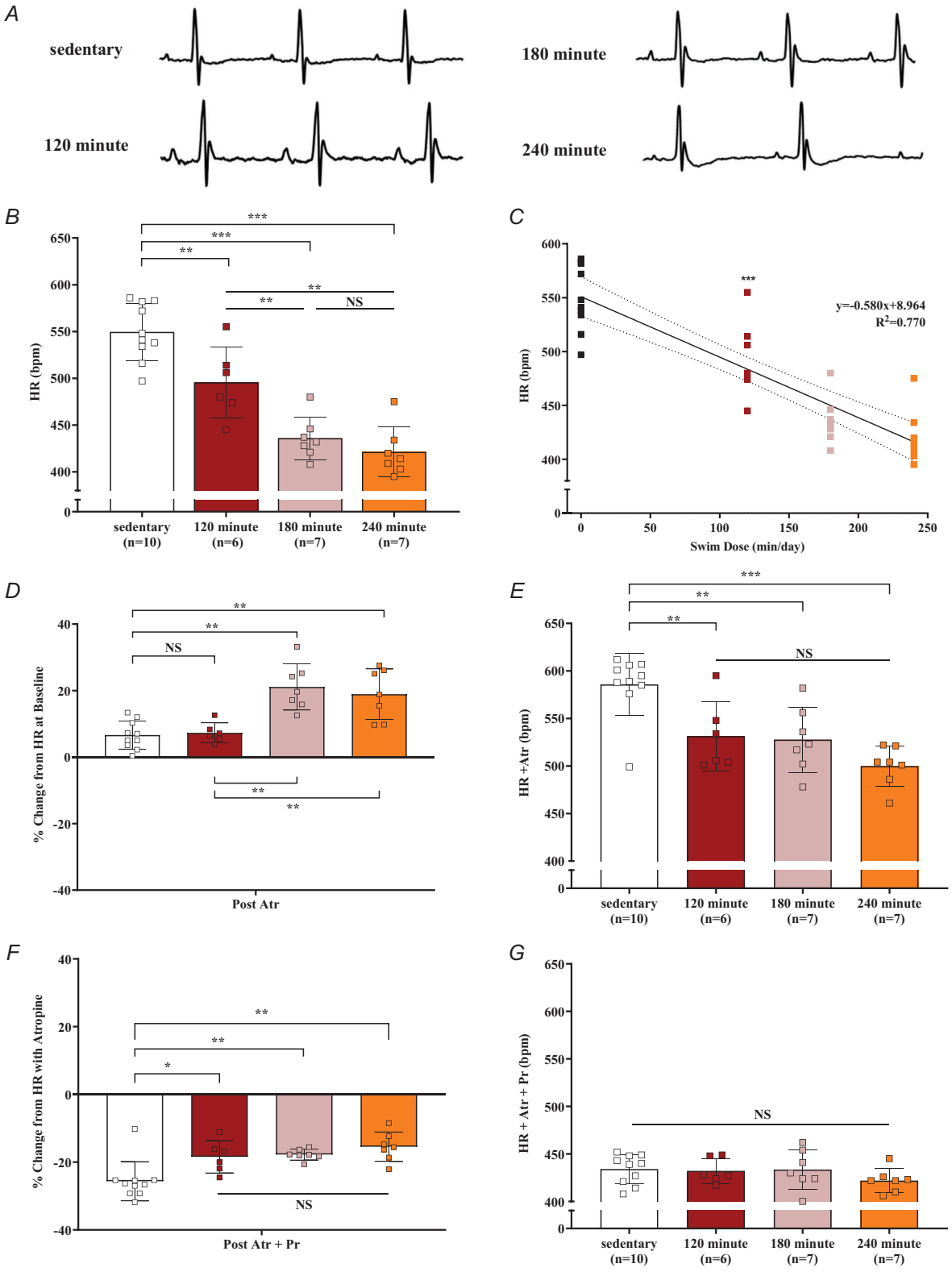

Figure 5. Effect of swim training on HRs and cardiac autonomic regulation
A, representative 0.2 s surface ECGs at baseline (Bl) for the control and swim groups. *B*, baseline resting HRs and (*C*) corresponding linear regression analysis. *D*, percentage change in HR from baseline to atropine (Atr) administration. *E*, HRs following parasympathetic inhibition via Atr. *F*, percentage change in HR from Atr to Atr and propranolol (Pr) administration. *G*, HRs following parasympathetic and sympathetic inhibition via Atr and Pr (i.e. complete auto-

nomic blockade). The *n* values presented in (*B*), (*E*) and (*G*) indicate the number of mice used throughout the figure. Data are the mean ± SD. *$P < 0.05$, **$P < 0.01$, ***$P < 0.0001$, using a one-way ANOVA with Tukey's multiple comparisons tests or simple linear regression analysis. [Colour figure can be viewed at wileyonlinelibrary.com]

Table 2. Physical ventricular parameters of mice swim-trained for variable daily durations

	Sedentary (control)	120 min (60 min × 2)	180 min (90 min × 2)	240 min (120 min × 2)
Body parameters, *n*	5	6	7	5
Body weight (g)	42 ± 3	40 ± 2	39 ± 2	39 ± 3
Tibia length (mm)	19.2 ± 0.2	19.5 ± 0.4	19.3 ± 0.3	19.3 ± 0.3
Ventricle weight (mg)	151 ± 10	170 ± 15	158 ± 14	173 ± 8*
Ventricle/body weight (mg g^{-1})	3.6 ± 0.3	4.2 ± 0.4*	4.1 ± 0.4	4.5 ± 0.4*
Ventricle/tibia length (mg mm^{-1})	7.9 ± 0.5	8.7 ± 0.9	8.2 ± 0.7	9.0 ± 0.3
Echocardiography, *n*	12	13	17	22
LVD_d (mm)	4.3 ± 0.2	4.5 ± 0.2	4.6 ± 0.2*	4.6 ± 0.2*
LVD_s (mm)	2.7 ± 0.2	3.0 ± 0.1*	3.1 ± 0.1*	3.2 ± 0.2*
EF (%)	67 ± 3.4	61 ± 2.9*	61 ± 2.6*	59 ± 3.6*
FS (%)	37 ± 0.8	32 ± 2.0*	32 ± 1.8*	31 ± 2.5*
LVPWTh (mm)	0.79 ± 0.03	0.77 ± 0.02	0.73 ± 0.05*	0.72 ± 0.04*
HR (beats min^{-1})	534 ± 28	461 ± 35*	432 ± 23*	423 ± 53*

LVD_d, left ventricular diastolic diameter; LVD_s, left ventricular systolic diameter; EF, ejection fraction; FS, fractional shortening; LVPWth, left ventricular posterior wall thickness; HR, heart rate. The *n* value shown presents number of mice included. Data presented as the mean ± SD.
*$P < 0.05$, compared with sedentary mice using one-way ANOVA with Tukey's multiple comparisons tests.

mimicking the mild physiological hypertrophy seen in endurance athletes (Morganroth, 1975) and there were no differences (VW/BW, $P = 0.382$ and VW/TL, $P = 0.254$) between the swim groups. In addition, one-way ANOVA comparisons of echocardiographic data showed that exercised mice had larger ($P < 0.001$) left ventricular (LV) end-systolic and end-diastolic diameters (volumes) compared to sedentary mice, although differences in end-diastolic diameter did not quite reach significance ($P = 0.061$) between the sedentary and 120 min mice.

Swim-trained groups also showed reductions ($P < 0.001$) both in fractional shortening (FS) and ejection fraction (EF) compared to the controls (Table 2), as seen in athletes (Conti et al., 2021) and as previously reported in exercised mice (Aschar-Sobbi et al., 2015). However, the rate of LV pressure development (dP/dt_{max}) at baseline (before dobutamine treatment) was the same ($P = 0.642$, one-way ANOVA) between exercised and sedentary mice, with upward trends ($P = 0.086$) of increased LV pressure development for the swim groups compared to sedentary mice following dobutamine challenge (Table 3). Moreover, the absolute change in the rate of LV pressure development following dobutamine administration was significantly increased ($P = 0.016$ and $P = 0.003$, paired *t* tests) in the 180 and 240 min groups, but not ($P = 0.823$ and $P = 0.680$) in the sedentary and 120 min mice (Table 3), even though a Tukey's multiple comparisons test failed to reveal differences ($P = 0.177$) between the swim groups. These findings are consistent with a plateauing effect of exercise training on LV functional and structural remodelling (McNamara et al., 2019). Also, no differences ($P = 0.257$) in LV end-diastolic pressures were observed between groups, despite increased LV end-diastolic diameters with exercise training, consistent with physiological ventricular remodelling. Furthermore, the minimum rate of LV pressure development (dP/dt_{min}) did not differ between the sedentary controls and swim groups either at baseline ($P = 0.491$) or in the presence of dobutamine ($P = 0.153$) and no differences ($P = 0.344$) in dP/dt_{min} were seen within each group pre- and post-dobutamine (Table 3). It should also be noted that the absolute change in mean HRs with dobutamine were increased in the swim groups (using paired *t* tests) far more than in the sedentary controls (Table 3), especially for the 180 and 240 groups. As a result, HRs following the dobutamine challenge were indistinguishable ($P = 0.155$) between groups, showing that reductions in resting HR do not impair cardiac contractility with exercise training, as seen with human athletes (Borresen & Lambert, 2008). Together, our data are consistent with the ventricular remodelling seen in endurance-trained individuals (Claessen et al., 2018) characterized by small reductions in EF with maintained or improved contractile and chronotropic reserve as assessed using a dobutamine challenge.

Table 3. Functional ventricular parameters of swim-trained mice

	Sedentary (control)	120 min (60 min × 2)	180 min (90 min × 2)	240 min (120 min × 2)
Haemodynamics, *n*	4	4	4	4
MAP (mmHg)	82 ± 11	78 ± 5	91 ± 14	92 ± 19
LVPs (mmHg)	79 ± 10	77 ± 9	91 ± 12	91 ± 14
LV ESP (mmHg)	81 ± 7	78 ± 10	91 ± 12	85 ± 20
LV EDP (mmHg)	20 ± 2	16 ± 3	17 ± 2	17 ± 3
LV $+dP/dt_{max}$ (mmHg s^{-1})	9584 ± 899	8816 ± 852	9945 ± 1276	8567 ± 2551
LV $-dP/dt_{min}$ (mmHg s^{-1})	−8706 ± 1005	−8005 ± 498	−9810 ± 1644	−8930 ± 2515
LV $+dP/dt_{max}$ + Dob (mmHg s^{-1})	10 500 ± 1018	10 272 ± 1407	13 363 ± 1428	12 988 ± 2660
LV $-dP/dt_{min}$ + Dob (mmHg s^{-1})	−7991 ± 852	−8138 ± 863	−9431 ± 1352	−9424 ± 1087
HR + Dob (beats min^{-1})	596 ± 41	632 ± 27	650 ± 35	625 ± 32
Δ in dP/dt_{max} with Dob (mmHg s^{-1})	916 ± 280	1456 ± 785	3418 ± 2277†	4421 ± 2681†
Δ in dP/dt_{min} with Dob (mmHg s^{-1})	715 ± 386	−133 ± 506	378 ± 1114	−494 ± 1453
Δ in HR with Dob (beats min^{-1})	72 ± 20	90 ± 53†	135 ± 78†	139 ± 34†

MAP, mean arterial pressure; LVPs, left ventricular systolic pressure; LV ESP, left ventricular end-systolic pressure; LV EDP, left ventricular end-diastolic pressure; LV $+dP/dt_{max}$, maximum rate of left ventricular pressure development; LV $-dP/dt_{min}$, minimum rate of left ventricular pressure development; + Dob, dobutamine challenge. The *n* values shown presents the number of mice included. Data presented as the mean ± SD.
* $P < 0.05$, compared to sedentary mice using one-way ANOVA with Tukey's multiple comparisons tests.
† $P < 0.05$, compared within individual groups before and after dobutamine administration using paired *t* tests.

Dose-dependent arrhythmia inducibility in swim-trained mice

We next investigated the impact of daily exercise dose on atrial and ventricular arrhythmia inducibility using programmed stimulation protocols introduced with octapolar catheters inserted into the right atria and right ventricle via the jugular vein. Both atria and ventricular arrhythmias were defined as reproducible bouts of chaotic activation lasting >10 s in the region of interest. Figure 6*A* shows representative recordings when the atrial leads are stimulated in a sedentary (left) and a 240 min swim mouse (right) at the end of the training period. Although AF was not inducible in sedentary mice (0/19), the incidence of sustained atrial arrhythmias was greater ($P = 0.005$, Fisher's exact test) in the swim-trained mice compared to the non-exercised controls (Fig. 6*B*). Specifically, detailed comparisons revealed that AF inducibility did not differ between the controls and 120 min group (3/17, $P = 0.232$) but increased in the 180 min (9/26, $P = 0.016$) and 240 min group (7/19, $P = 0.013$). When sustained AF occurred, the duration of the arrhythmic events did not differ ($P = 0.209$, one-way ANOVA) between the exercise groups (Fig. 6*C*). By contrast, ventricular arrhythmias could not be evoked in either sedentary or exercised mice.

To better understand the potential mechanisms for the influence of daily exercise dose on AF vulnerability, we assessed atrial electrical refractoriness, hypertrophy and fibrosis because these factors are known to play central roles in AF mechanisms (Jalife & Kaur, 2015). To determine the role of atrial refractoriness in AF risk with exercise, we measured the AERPs in anaesthetized mice by delivering a series of pulses followed by an extrastimulation of increasing delay until capture (for details, see Methods). Despite the dependence of AF on daily exercise dose, AERPs were similar ($P = 0.229$) between sedentary and exercised mice (Fig. 7A). Because elevated cardiac parasympathetic activity, as observed in our exercise mice, is known to promote AF through reducing AERPs (Guasch et al., 2018), especially in athletes (Mont, 2002), we explored the effects of atropine (2 mg kg^{-1}) on AF inducibility. Consistent with our HR analyses showing increased cardiac parasympathetic nerve activity with exercise, we found that cardiac parasympathetic blockade produced AERP prolongation within each group ($P < 0.001$, paired *t* tests), with the atropine-sensitivity being greatest in the swim groups compared to sedentary mice ($P < 0.001$, one-way ANOVA), with no differences ($P = 0.871$) between the swim groups using Tukey's multiple comparisons tests (Fig. 7*B*). Importantly, AERP prolongation abbreviated atrial arrhythmia durations and reduced AF inducibility in the subsets of inducible mice tested with atropine (0/3, 2/6 and 2/7 for the 120, 180 and 240 min groups, respectively) (Fig. 7*C* and *D*), consistent with previous findings (Aschar-Sobbi et al., 2015; Lakin et al., 2019). Taken together, these results establish that parasympathetic nerve activity influences inducibility and arrhythmia durations, although differences in AERP are not solely responsible for enhanced AF vulnerability caused by increasing daily exercise dose.

The inability of atropine to eliminate AF in the 180 and 240 min groups, combined with the absence of AERP differences between groups despite variable AF inducibility, suggests that other factors are contributing to the increased AF vulnerability seen in mice with the greatest daily exercise dose. Because fibrosis is seen invariably in AF (Sohns & Marrouche, 2020), we assessed atrial collagen content using PSR staining in the left atrial appendages and LVs (Fig. 8*A*). These measurements revealed increased atrial fibrosis ($P < 0.001$, one-way ANOVA) in each swim group compared to sedentary mice, with linear regression analyses establishing a strong dependence of increased ($R^2 = 0.704$, $F_{1,26} = 61.8$, $P < 0.001$) fibrosis on the daily exercise amount (Fig. 8*B* and *C*). The dose dependence of atrial fibrosis was also observed primarily in pericapsular ($R^2 = 0.704$, $F_{1,26} = 61.92$, $P < 0.001$) regions of the atria rather than interstitial ($R^2 = 0.469$, $F_{1,26} = 22.97$, $P < 0.001$) using linear regression analysis. However, it should be noted that one-way ANOVA analyses did not reveal differences in collagen between the exercised groups ($P = 0.184$ for interstitial and $P = 0.228$ for pericapsular) (Fig. 8*D*–*G*). Interestingly, total collagen content was additionally increased ($P < 0.025$, one-way ANOVA) in the LV free wall for swim groups relative to the controls with linear regression analyses showing a small

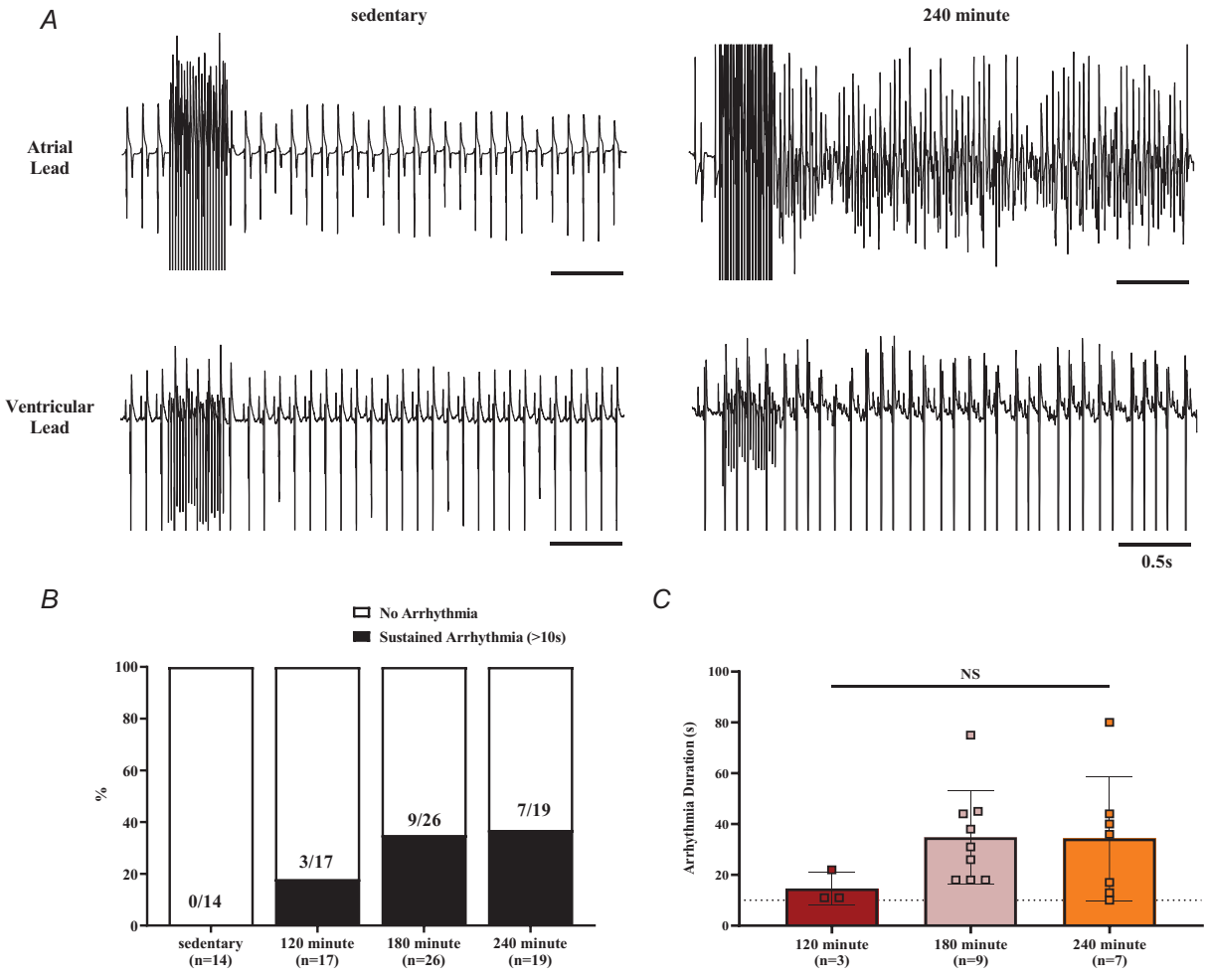

Figure 6. Atrial fibrillation inducibility increases with daily exercise dose
We delivered rapid atrial programmed stimulations *in vivo* to assess arrhythmia susceptibility. *A*, representative electrograms illustrate tracings from a sedentary mouse in sinus rhythm and a 240 min mouse experiencing an atrial arrhythmia following programmed stimulation. The top tracings show an intracardiac lead from the mid atria and the bottom shows the simultaneously recorded ventricular lead. *B*, percent of mice that had sustained and reproducible arrythmia inducibility (>10 s). Note the percentage increases with the prolongation of daily swim duration. *C*, the average arrhythmia duration in each group, including only the mice that were inducible in (*B*). The dotted line represents the 10 s threshold for classification of a sustained arrythmia. The *n* values indicate the number of mice included. Data represented as the mean ± SD, using a one-way ANOVA with Tukey's multiple comparisons tests. [Colour figure can be viewed at wileyonlinelibrary.com]

dependence ($R^2 = 0.269$, $F_{1,25} = 9.22$, $P = 0.006$) on daily exercise dose (Fig. 9), yet the amount of fibrosis is considerably smaller compared to left atrial appendages.

In addition to atrial fibrotic remodelling, atrial hypertrophy is another exercise-induced atrial change linked to AF vulnerability in endurance athletes (Turagam et al., 2015). As such, linear regression analyses revealed that the (wet) atrial weights normalized to either body weight (i.e. AW/BW) or tibia length (i.e. AW/TL) progressively increased (AW/BW: $R^2 = 0.484$, $F_{1,21} = 19.65$, $P < 0.001$ and AW/TL: $R^2 = 0.461$, $F_{1,21} = 17.97$, $P < 0.001$) as daily exercise dose was prolonged (Fig. 10*B* and *D*), mirroring the progressive atrial (but not ventricular) hypertrophy observed in humans with increasing training duration (McNamara et al., 2019). Consistent with the linear regression analyses, we found AW/BW and AW/TL were increased in the 180 min ($P = 0.004$ and $P = 0.004$) and 240 min ($P = 0.006$ and $P = 0.007$) groups, but not in the 120 min mice ($P = 0.699$ and $P = 0.921$) compared to the controls using one-way ANOVA (Fig. 10*A* and *C*). Moreover, the AW/BW and AW/TL were increased in the 180 min ($P = 0.031$ and $P = 0.012$) and 240 min ($P = 0.042$ and $P = 0.019$) groups relative to the 120 min mice.

Atrial macrophage infiltration in swim-trained mice

Because tissue fibrosis and hypertrophy (Jalife & Kaur, 2015) are invariably associated with increased inflammation (Engelmann & Svendsen, 2005), including in exercised mice (Aschar-Sobbi et al., 2015), we also quantified macrophage numbers in histological cardiac sections using F4-80 antibodies. Macrophage counts normalized to tissue area (i.e. mm^2) were elevated in the 180 min and 240 min groups relative to the controls

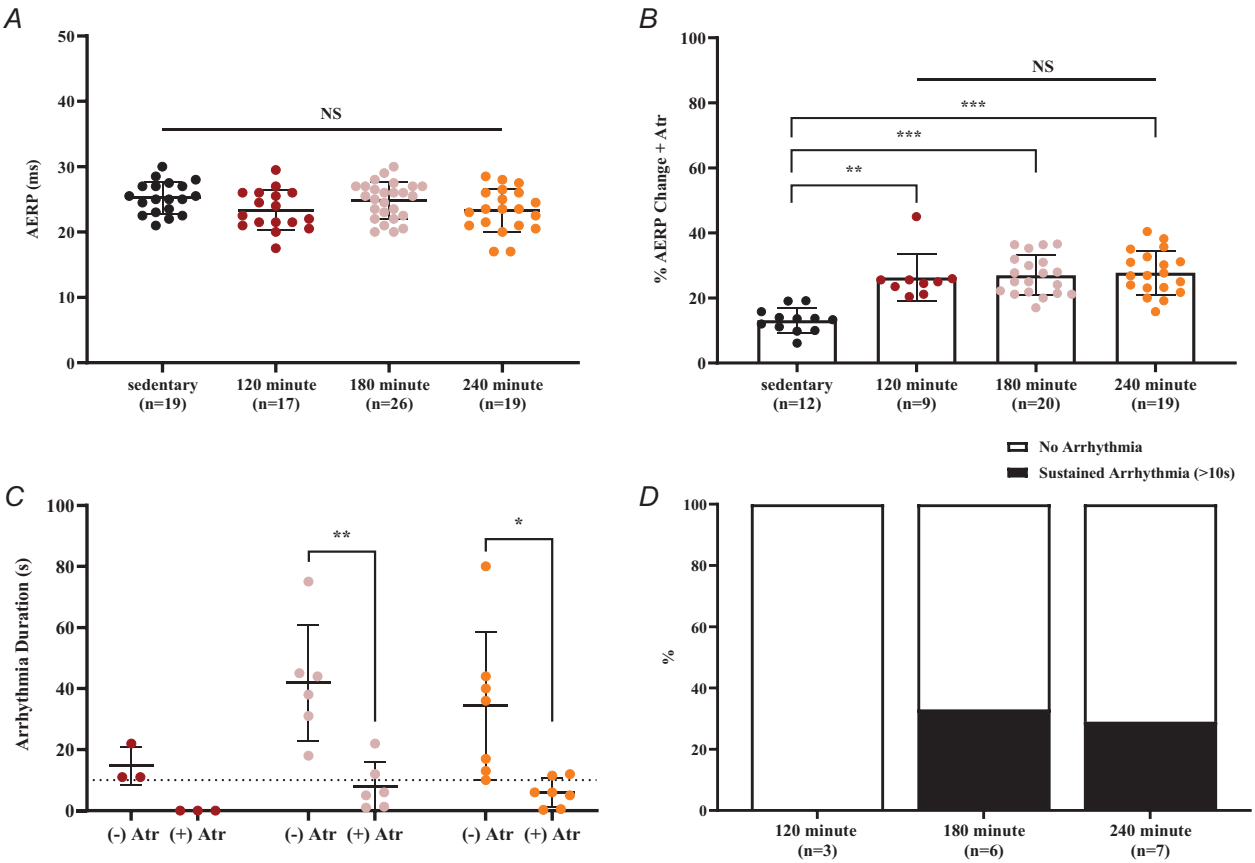

Figure 7. Effects of atropine on atrial refractoriness and AF susceptibility in swim-trained mice
To investigate the role of training-induced elevated vagal tone in AF susceptibility, we assessed the refractory periods and AF durations following I.P. injections with 2 mg kg^{-1} atropine of anaesthetized mice *in vivo*. *A*, atrial effective refractory period (AERP) in the right appendage at baseline. *B*, change in AERP following parasympathetic inhibition via atropine (Atr). *C*, arrhythmia durations and (*D*) percent inducibility following atropine injection in a subset of the exercised mice that were previously inducible (i.e. had AF events >10 s following programmed stimulation). In (*C*), the 120 min mice are red ($n = 3$), 180 min mice are pink ($n = 6$) and 240 min mice are orange ($n = 7$). For all other panels, the n values indicate the number of mice used. Data presented as the mean ± SD. $^*P < 0.05$, $^{**}P < 0.01$, $^{***}P < 0.0001$ using one-way ANOVA with Tukey's multiple comparisons tests (*A* and *B*) or paired t tests (*C*). [Colour figure can be viewed at wileyonlinelibrary.com]

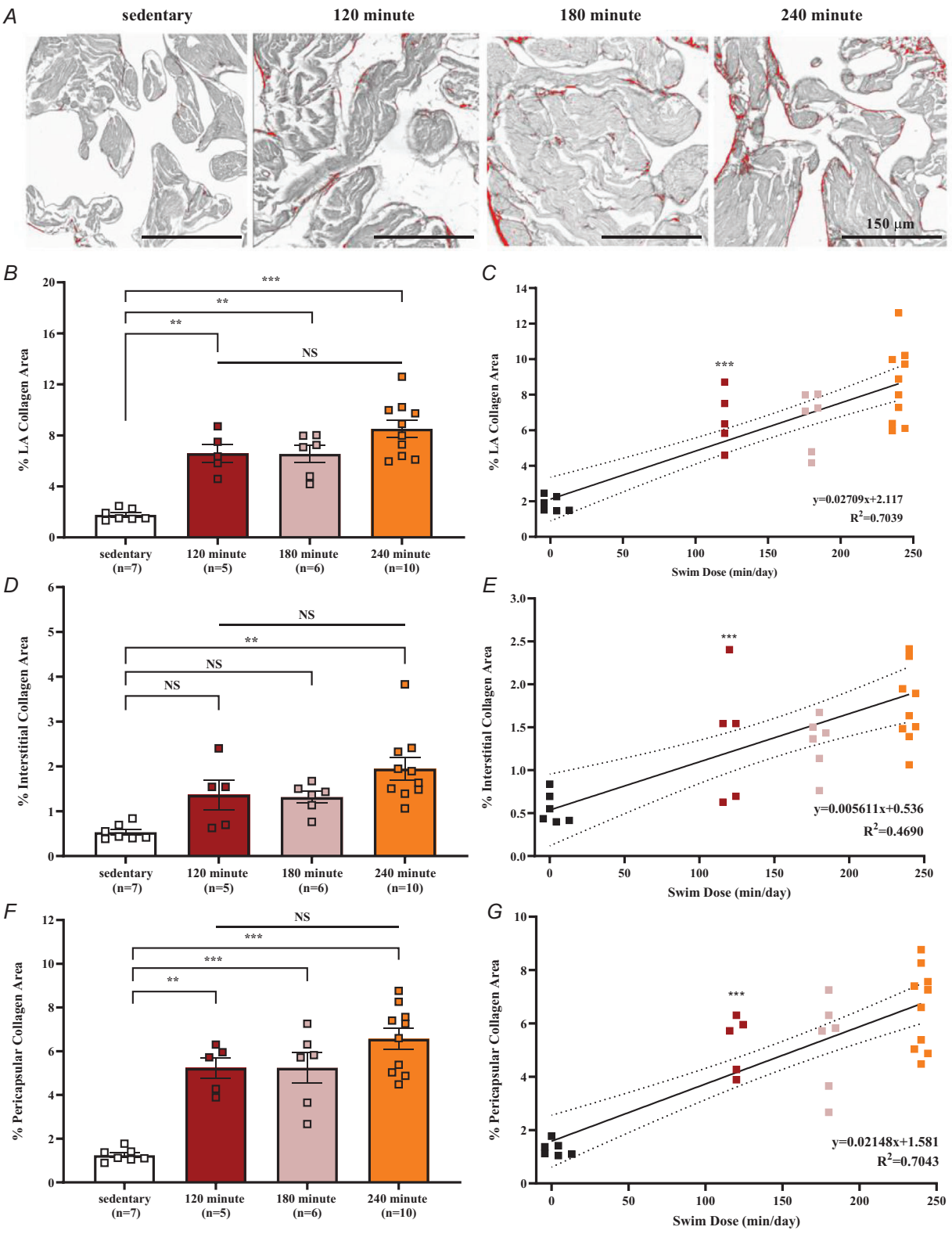

Figure 8. Swim training at variable daily durations induces atrial fibrosis predominately in pericapsular regions

A, representative images of the left atrial appendage where collagen was identified using picrosirius red and imaged using a slide-scanner brightfield microscope at 20×. *B*, quantification of total atrial collagen content and (*C*) simple linear regression analysis based on selecting and counting pixel brightness, standardized to total tissue. Tissues were then separately analyzed for collagen in the interstitial and pericapsular regions. *D*, percent interstitial collagen

deposition and (*E*) the corresponding linear regression analysis. *F*, percent pericapsular collagen deposition and (*G*) the corresponding linear regression analysis. The *n* values in (*B*), (*D*) and (*F*) indicate the number of mice included. Data are the mean ± SD. $^{*}P < 0.05$, $^{**}P < 0.01$, $^{***}P < 0.0001$ using a one-way ANOVA with Tukey's multiple comparisons tests or simple linear regression analysis. [Colour figure can be viewed at wileyonlinelibrary.com]

($P = 0.045$ and $P < 0.001$) and the 120 min group ($P = 0.021$ and $P = 0.020$) using one-way ANOVA with Tukey's multiple comparisons tests (Fig. 11*B*). Moreover, linear regression analyses showed that the total macrophage numbers per area in the left atrial appendages increased substantially ($R^2 = 0.599$, $F_{1,21} = 31.32$, $P < 0.001$) as daily training duration increased (Fig. 11*C*). By contrast, we found no difference ($P = 0.264$, one-way ANOVA) in macrophage numbers between control and swim groups in the ventricles with no dose dependency as assessed using linear regression analyses ($R^2 = 0.079$, $F_{1,10} = 0.86$, $P = 0.375$) (Fig. 11*E* and *F*). Importantly, atria showed a 2.5-to 3-fold greater increase in macrophages compared to the LV with exercise, establishing chamber-unique inflammatory cell responses to exercise.

Discussion

Although regular physical activity protects against CV disease and mitigates AF incidence (Pathak et al., 2015), high-intensity endurance sport, particularly in veteran and elite athletes, increases AF incidence (Elliott et al., 2018). Indeed, there is growing epidemiological evidence that repetitive bouts of high-intensity exercise and competition (≥12–15 METs) are associated with AF risk (Franklin et al., 2020). Based on these findings, it has been suggested that the incidence of AF has a J-shaped dependence on exercise 'dose', where the benefits of low-to-moderate exercise to reduce AF prevalence yield to increased AF incidence in cohorts performing very high volumes of intense endurance exercise (Buckley et al., 2020). Unfortunately, establishing an absolute risk of AF with exercise is difficult given the differences

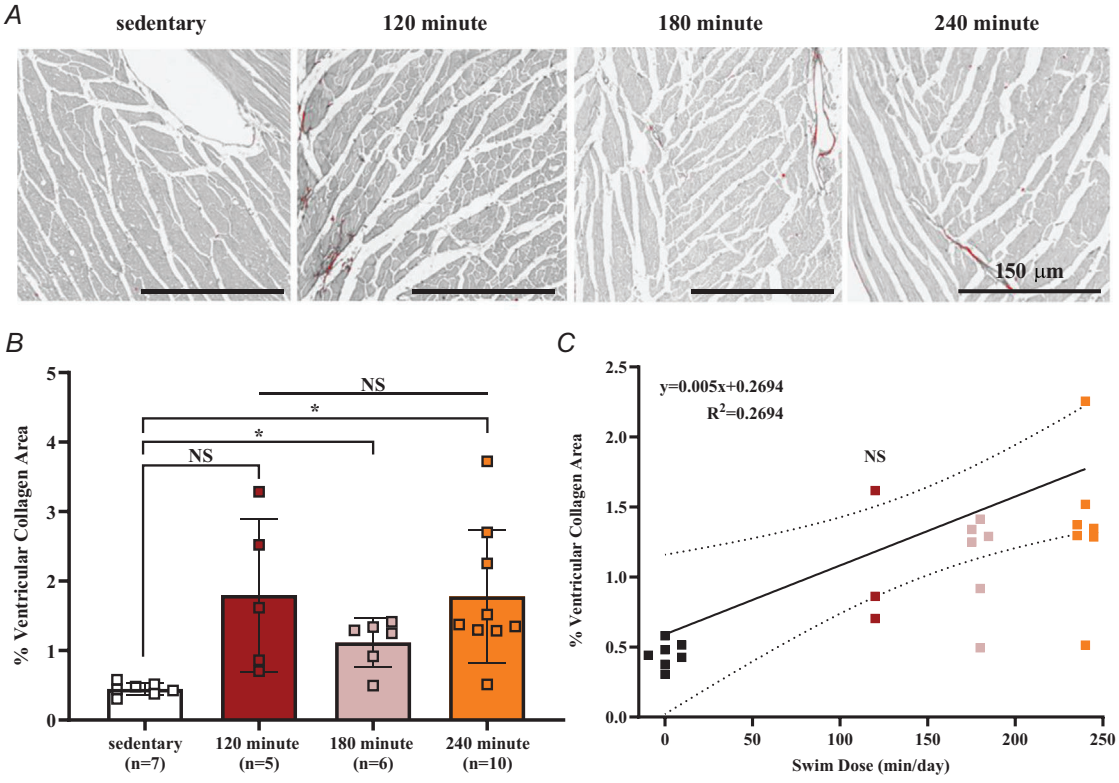

Figure 9. Swim training induced minimal ventricular fibrosis
Left ventricular collagen content was identified using picrosirius red and imaged using a slide-scanner brightfield microscope at 20×. *A*, representative images of collagen content in the left ventricular free wall. *B*, quantification of ventricular collagen involved selecting and counting pixels based on brightness (i.e. thresholding). *C*, linear regression analysis of swim dose and ventricular collagen data. The *n* values in (*B*) indicate the number of mice included. Data are the mean ± SD, $^{*}P < 0.05$, using one-way ANOVA with Tukey's multiple comparisons tests or simple linear regression analysis. [Colour figure can be viewed at wileyonlinelibrary.com]

in study methodologies, with most studies relying on self-reporting to characterize exercise intensities and volumes (Gerche & Schmied, 2013). Our studies were designed to assess quantitatively the impact of daily exercise dose on atrial remodelling and AF vulnerability using our mouse swimming model. We previously reported that CD1 mice, which instinctively swim against water currents, develop adverse atrial remodelling and enhanced AF vulnerability after 6 weeks of swimming for 180 min day^{-1} (divided into two sessions) (Aschar-Sobbi et al., 2015). To explore the effects of exercise dose, we initially attempted to vary the intensity by adjusting the water current velocities but found that CD1 mice self-regulate their swimming effort. Given our mice naturally swim at high intensities (~85–90% $\dot{V}_{O_2\,max}$) (Aschar-Sobbi et al., 2015), we achieved our objectives by varying the daily swim duration (i.e. 120, 180 or 240 min day^{-1}) and comparing the mice after all three groups had performed equivalent absolute work during swimming (estimated by the total O_2 consumed). To reach ~700 L O_2 kg^{-1} when training, mice exercising for 120 min per day swam for ~45 days, whereas mice swimming for 180 or 240 min required ~30 or ~22.5 days, respectively. This tight inverse relationship between daily swim duration and the number of training days might initially be unexpected given that the average $\dot{V}_{O_2}$ values increased more rapidly each week with prolonged daily swim duration (i.e. a slope of 56, 149 and 266 $\Delta\dot{V}_{O_2}$ week^{-1} for the 120, 180 and 240 min groups, respectively), indicating a more rapid rate of aerobic conditioning. However, replotting the mean $\dot{V}_{O_2}$ as a function of hours spent swimming eliminated differences between the groups. Moreover (and consequently), the mean $\dot{V}_{O_2}$ was indistinguishable between the exercise groups at the end of the training period but were all elevated relative to the sedentary group. Thus, the exercise groups showed similar extents of aerobic conditioning. Consistent with this conclusion, we observed comparable increases in mitochondrial oxidative capacity for the three exercise groups relative to sedentary mice, which parallels human observations (Dumke et al., 2009). Indeed, prolonged engagement in excessive endurance activity is known to impose repetitive haemodynamic stress on the heart and skeletal muscle, with the elevated skeletal muscle mitochondrial content (i.e. elevated COX enzyme activity) suggesting enhanced fatigue resistance and maintenance

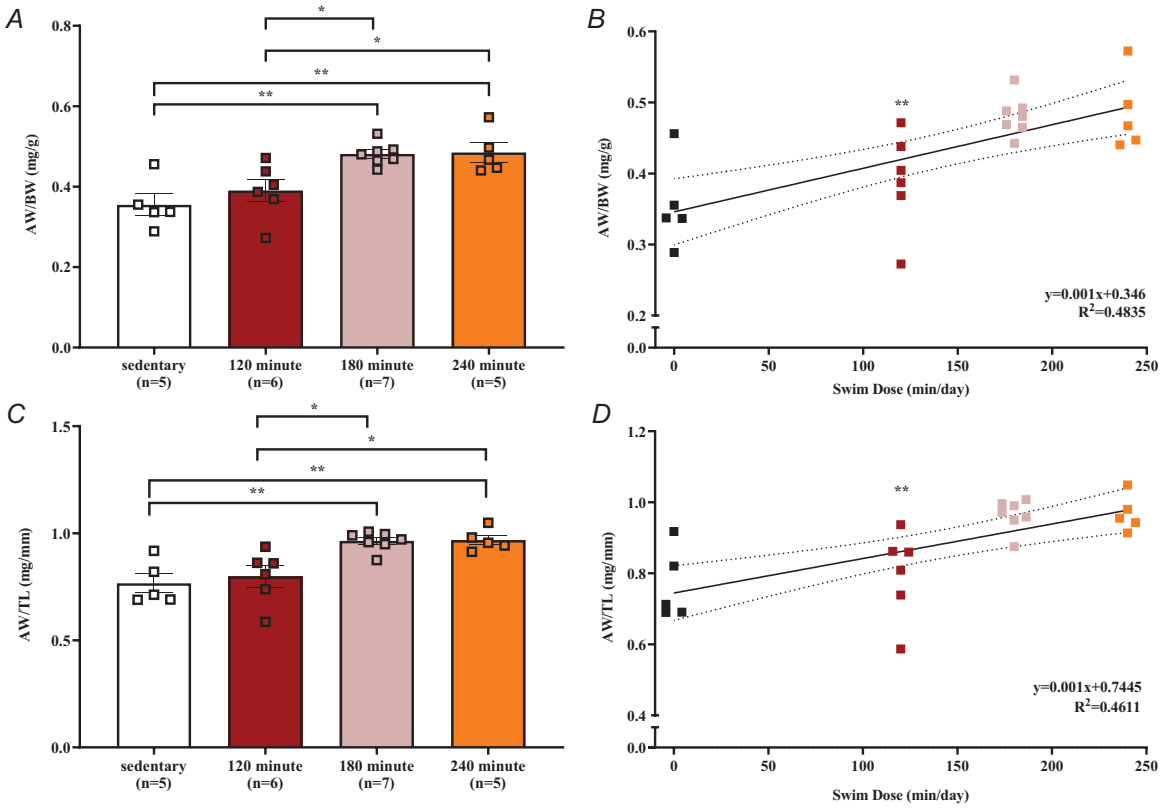

Figure 10. Swim training at variable daily durations induces atrial hypertrophy
A, atrial weight normalized to body weight (AW/BW) and (*B*) the corresponding linear regression analysis. *C*, atrial weight normalized to tibia length (AW/TL) and (*D*) the corresponding linear regression analysis. The *n* values in (*A*) and (*B*) indicate the number of mice included throughout. Data are the mean ± SD. $^{*}P < 0.05$, $^{**}P < 0.01$, $^{***}P < 0.0001$ using a one-way ANOVA with Tukey's multiple comparisons tests or simple linear regression analysis. [Colour figure can be viewed at wileyonlinelibrary.com]

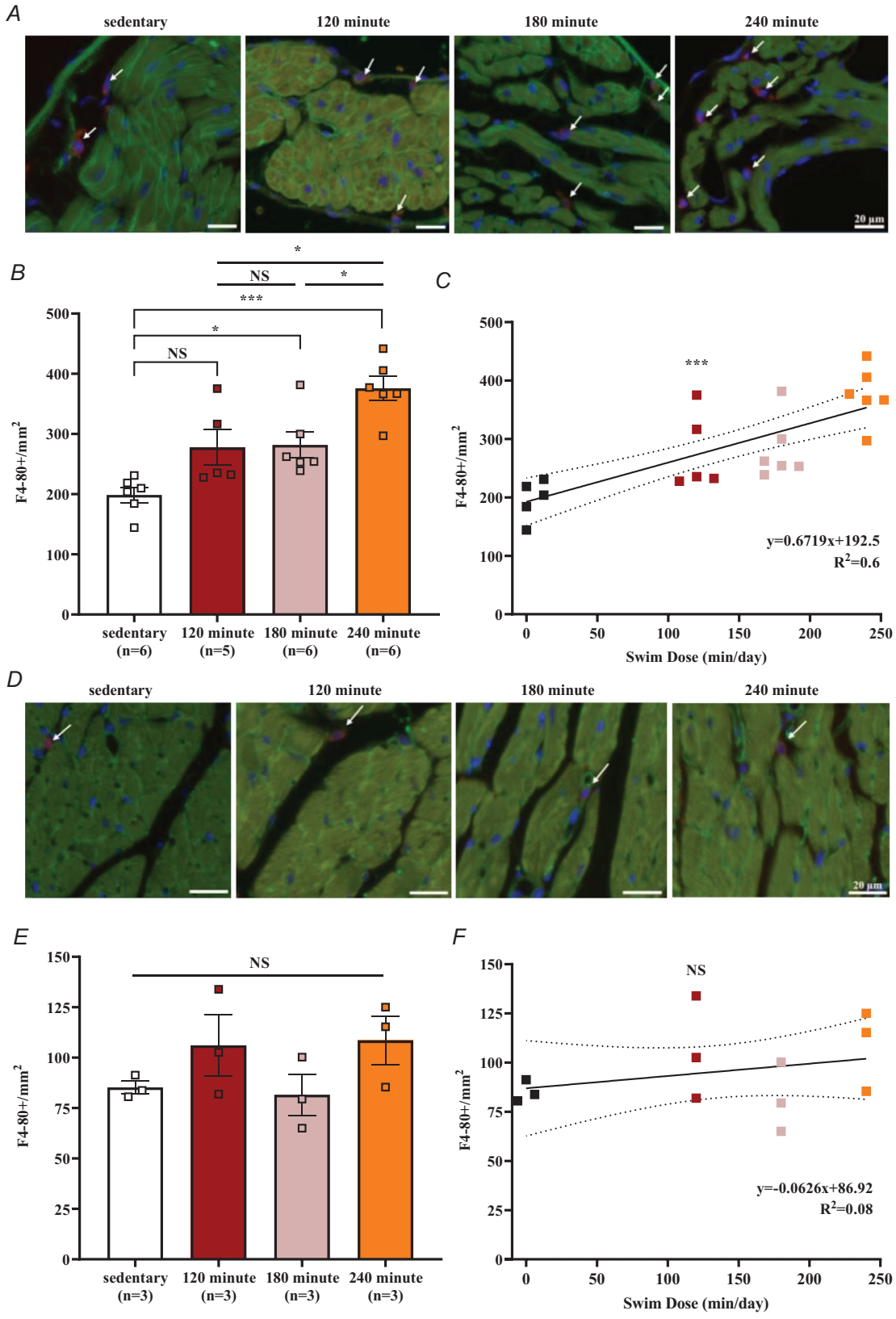

Figure 11. Swim training at daily variable durations induces atrial not ventricular inflammation
The presence of macrophages was investigated using immunohistology assessment with antibodies against F4-80, a cell surface glycoprotein expressed by macrophages in mice. *A*, representative individual images of the left atrial

appendage and (*D*) left ventricular free wall taken with a slide-scanning confocal microscope at 20×; positive cells co-stained for DAPI (indicating the nuclei) and F4-80 (macrophage marker). *B* and *E*, number of macrophages per mm^2 with (*C* and *F*) the corresponding linear regression analysis. The *n* values in (*B*) and (*D*) indicate the number of mice included for atrial and ventricular assessments, respectively. Data are the mean ± SD. $^*P < 0.05$, $^{**}P < 0.01$, $^{***}P < 0.0001$, using one-way ANOVA with Tukey's multiple comparisons tests or simple linear regression analysis. [Colour figure can be viewed at wileyonlinelibrary.com]

of higher power output during endurance exercise (Dumke et al., 2009), consistent with increased $\dot{V}_{O_2}$ as training progressed.

In conjunction with the changes in aerobic conditioning, all three exercised groups displayed similar, albeit small, reductions in FS and EF, as well as mild, indistinguishable ventricular dilatation (i.e. end-diastolic and end-systolic diameters) compared to sedentary mice, which mirrors the athlete's heart phenotype typically associated with endurance training (Claessen et al., 2018). The absence of differences in LV remodelling between the swim groups may reflect the equivalent work performed by the mice in each group during swimming or may represent a plateau effect of prolonged exercise on LV dilatation, as described previously in athletes (McNamara et al., 2019). In association with ventricular dilatation, exercised mice also displayed reduced FS (and thereby EF), possibly suggesting impaired cardiac contractility. However, baseline ventricular contractility (i.e. dP/dt_{max}) was not reduced in exercised mice compared to controls, whereas dP/dt_{max} increased in the 180 or 240 min swim mice after dobutamine treatment. This pattern parallels the improved ability of endurance athletes to recruit greater cardiac reserve during exercise via adrenergic-dependent augmented cardiac contractility despite reduced FS and EF at rest (Mier et al., 1997).

Our findings demonstrate a novel interplay between electrical and structural changes in atria that appear to progressively predispose to AF inducibility as daily exercise dose is increased. For example, unlike the skeletal muscle and ventricular adaptations to exercise, the degree of HR reduction and related cardiac parasympathetic autonomic activity (as assessed in anaesthetized mice) increased as daily swim durations were prolonged. This augmentation of cardiac parasympathetic activity by increased exercise dose correlated with progressive enhancements of atrial arrhythmia inducibility, without affecting ventricular arrhythmia susceptibility, whereas parasympathetic blockade with atropine decreased AF susceptibility. Presumably, the effects of atropine on AF inducibility are related to increased AERP (Guasch et al., 2018) resulting from reduced $I_{K,Ach}$ and elevated I_{Ca} (Rebecchi et al., 2021), as well as possible mitigation of heterogeneity in atrial refractoriness arising from inhomogeneous vagal nerve innervation, seen in AF (Yeh et al., 2007). These observations in mice align nicely with the elevated vagal tone in endurance athletes (Gourine & Ackland, 2019), as well as the strong connection between vagal tone and AF (Guasch et al., 2018). It could be argued that the relevance of our studies to athletes are limited because our assessments of autonomic nerve activity in mice were performed under anaesthesia, which can affect autonomic regulation of heart function (Janssen et al., 2004). However, the effects of autonomic blockers on HR in anaesthetized mice are effectively indistinguishable from measurements in conscious (implanted) mice (Ishii et al., 1996; Uechi et al., 1998). Additionally, we have demonstrated previously that anaesthetized and conscious mice show similar circadian fluctuations in baseline HR, which are dominated by the parasympathetic nervous system, with these fluctuations increasing profoundly in exercised mice (Barazi et al., 2021). These observations appear to be particularly relevant because the AF incidence in athletes shows a strong circadian dependence (Li et al., 2010), as does AF in paroxysmal AF patients (Yamashita et al., 1997).

The absence of differences in AERP between the exercise groups, despite increases in AF vulnerability as daily exercise duration is prolonged as well as the observation that the 180 and 240 min groups remained vulnerable to AF induction after blockade of cardiac parasympathetic nerve activity, supports the conclusion that non-electrical structural factors must also contribute to AF vulnerability. In this regard, atrial hypertrophy and chamber enlargement are hallmarks of athlete's hearts (Król et al., 2016) that can facilitate cardiac output during exercise, but promotes simultaneously AF by extending conductive path lengths and altering cellular architecture (Neuberger et al., 2006). In our studies, we observed marked atrial hypertrophy (measured as atrial weight normalized to either body weight or tibia length), which increased progressively with prolonged daily swim durations and correlated well with AF inducibility. A second important structural change seen commonly in AF, and arrhythmias more broadly, is atrial fibrosis (Dzeshka et al., 2015), which slows electrical propagation by impeding conduction, as well as possibly loading capacitively cardiomyocytes (Miragoli & Glukhov, 2015). As reported previously in rodent exercise models (Aschar-Sobbi et al., 2015; Benito et al., 2011), as well as in Masters athletes engaged in endurance sports (i.e. running, cycling, Nordic skiing) (Peritz et al., 2020), we observed atrial fibrosis in all swim-trained mice with regression analyses showing that atrial fibrosis increases generally as daily exercise is prolonged, though fibrosis differences between the exercise groups did not reach significance and did not

correlate as strongly with AF inducibility as atrial hypertrophy. Interestingly, atrial fibrosis was most prominent in the pericapsular regions, which may be designed teleologically as an adaptative response to preserve structural integrity following haemodynamic stress and atrial stretch associated with exercise (see below). This adaptive response may be physiologically relevant because of the atria's endocrine role in regulating body fluids by releasing atrial natriuretic peptide in response to stretch, which is linked to atrial-specific fibrosis (Rahmutula et al., 2019).

The basis for the increased hypertrophy and fibrosis in atria, but not ventricles, in swim-exercised mice is undoubtedly complex. To aid our discussion, it is helpful to first consider the physiological responses of the cardiovascular system to the increased demand in blood flow during exercise. Many inter-dependent cardiovascular changes occur to ensure adequate tissue perfusion during exercise (Joyner & Casey, 2015), such as elevations in peak systolic blood (arterial) pressure (originating primarily from abbreviated systolic periods and elevated cardiac contractility (Mier et al., 1997)) and elevated cardiac output (achieved by increased stroke volume and autonomic-dependent elevations in HR). Increased stroke volume arises primarily from increased venous (and LV end-diastolic) filling pressures (i.e. the Starling effect), which we have demonstrated previously occurs in exercising mice using implanted pressure telemetry devices (Lakin et al., 2021), mimicking responses in humans to exercise (Reeves et al., 1990). In particular, LV end-diastolic filling pressure rises to 51 ± 3 mmHg within the first 2 mins after mice begin swimming. Thereafter, filling pressures fall to 26 ± 4 mmHg and remain stable for about 45 min, only to rise steadily thereafter for the remainder of the swim (reaching 30 ± 3 mmHg at 60 min, 37 ± 5 mmHg at 90 min and 44 ± 2 mmHg at 120 min). Because the compliance of atria is more than 2-fold greater than ventricles (Aschar-Sobbi et al., 2015), atria are expected to stretch far more than ventricles when filling pressures rise (Hamilton et al., 1994) and this cardiac stretch can activate many signalling pathways involved with hypertrophy, fibrosis and inflammation (De Jong et al., 2011). Together, these observations support the conclusion that pressure-mediated atrial stretch underlies the increased AF vulnerability, without parallel changes in ventricles, observed with prolonged daily swim durations. Additionally, because the degree of atrial hypertrophy paralleled AF vulnerability more clearly than fibrosis as exercise dose was increased, our data further suggests that the degree of hypertrophy may be of greater relevance in the promotion of AF with exercise dose than atrial fibrosis, although fibrosis undoubtedly enhances AF susceptibility in all groups. This speculation is consistent with many previous studies that have linked atrial hypertrophy to AF in athletes (Mont et al., 2008), whereas the involvement of fibrosis has been highly controversial (Małek & Bucciarelli-Ducci, 2020). Because previous studies have established that elevated filling pressure also occurs in humans during exercise (Reeves et al., 1990), it will be interesting to explore whether similar temporal changes in pressure during prolonged intense exercise also occur, as seen in our mouse model. Moreover, given that atrial hypertrophy is expected to be a beneficial cardiac adaptation to chronic exercise, targeting hypertrophy may represent a double-edged sword.

Although many stretch-activated factors and pathways could be critical, atrial inflammation may also be an integral feature of AF pathogenesis in athletes (Swanson, 2006). Consistent with this, we observed progressive increases in atrial macrophage accumulation with extended daily swim durations, and our previous mouse studies established a crucial role for the pleiotropic inflammatory cytokine, tumour necrosis factor (TNF), in atrial fibrosis and hypertrophy, along with AF susceptibility and inflammatory cell infiltrations (Aschar-Sobbi et al., 2015). The ∼3-fold greater macrophage infiltration in atria *vs.* ventricles in our swim mice is also consistent with human AF patients and rodent models that elicited AF using a combined hypertension, obesity and mitral valve regurgitation (three-hit) model, in which macrophages were the primary immune cells in atria associated with AF (Hulsmans et al., 2023). This suggestion appears to be particularly attractive because a previous study has demonstrated that elevated cardiac mechanical stress in mice involves mechanosensitive TRPV4 channels in macrophages (Nguyen et al., 2022), which are a primary source of TNF. However, we have shown recently that TNF elimination in atrial cardiomyocytes protects against exercise-induced atrial fibrosis, hypertrophy and macrophage infiltrations along with AF (Lakin et al., 2023). More studies are needed to assess the involvement of TNF along with other stretch-dependent pathways in the atrial response to daily exercise dose.

Scaling of exercise dose and responses from our mouse swim model to humans

Our findings establish that prolonging daily swim durations drives more adverse atrial changes and greater AF vulnerability, even after mice perform the same total work when swimming. We consider our study to be the first to quantitatively link daily exercise dose and AF risk in mice, consistent with previous human studies based on self-reporting (Gerche & Schmied, 2013). The relevance of our studies to the J-shaped dependence of AF incidence on exercise dose (Buckley et al., 2020) is not immediately obvious for several reasons. Previous studies in humans have concluded that AF incidence increased in endurance athletes who engage in ≥55 MET-h week^{-1} at intensities

of 15–20 METs (Franklin et al., 2020; Sharma et al., 2015). By definition, 1 MET is the $\dot{V}_{O_2}$ during rest and equals ∼210 mL O_2 kg^{-1} h^{-1} (Jetté et al., 1990), whereas ≥55 MET-h $week^{-1}$ of exercise is well above the levels recommended by the United States Physical Activity Guidelines for adults (Singh et al., 2020). Comparing these estimates to our exercised mice, we found that $\dot{V}_{O_2}$ levels reached 10 653 ± 192 mL O_2 kg^{-1} h^{-1} during swimming by the end of training. If we use the $\dot{V}_{O_2}$ of mice during sleep (i.e. ∼2300 mL O_2 kg^{-1} h^{-1}), swimming is estimated to require 4–5 METs in our exercised mice. Based on these estimates, only the 180 and 240 min groups exceeded the 55 MET-h $week^{-1}$ threshold linked to AF in humans (i.e. the exercise doses were 40–50, 60–75 and 80–100 MET-h $week^{-1}$ for the 120, 180 and 240 min groups, respectively), which aligns remarkably with the increased AF vulnerability and greater adverse atrial remodelling in these two groups. Moreover, Fisher's exact comparisons at baseline (without autonomic inhibitors) revealed that AF inducibility only increased in the 180 and 240 min swim groups compared to the controls. Additionally, AF was still inducible in the 180 and 240 min groups after atropine application. Together, our results support the conclusion that an exercise dose threshold is required to enhance AF vulnerability. Because one-way ANOVA comparisons also revealed that atrial hypertrophy was augmented in the 180 and 240 min groups only, whereas fibrosis increased in all exercised mice, compared to the controls, our works further suggest that differential atrial hypertrophy might be the primary determinant of AF vulnerability induced by exercise as a consequence of prolonged elevations in filling pressures with increased daily exercise duration.

Limitations

Previous studies have shown that anaesthesia can affect cardiac autonomic nerve activity, which needs to be considered when making inferences from our work on AF in athletes. However, as mentioned above, our assessments of autonomic nerve activity with blockers align remarkably well with previous results in conscious mice (Ishii et al., 1996; Uechi et al., 1998), which support our conclusion that cardiac parasympathetic activity is a factor in the increased AF vulnerability in mice. We also previously showed that circadian fluctuations in autonomic regulation of HR is dominated by the parasympathetic system and, because our assessments of AF vulnerability were limited to ZT16 to ZT22 (i.e. during their rest period), it is conceivable (and probable) that AF susceptibility would be quite different if our AF evaluations were performed at other times of day.

Our conclusions related to autonomic influences on the relationship between the exercise dose and AF vulnerability were based on the use of specific blockers to estimate autonomic nerve activity. However, we (Lakin et al., 2018) and others (Lujan et al., 2016) have shown that complex interactions exist between the parasympathetic and sympathetic systems, especially via a phenomenon called accentuated antagonism. Consequently, the cardiac responses to blockers do not directly translate one-to-one to corresponding measures of cardiac autonomic activity. Although these interactions, in principle, complicate our estimates of the regulation of heart function by the autonomic nervous system, their impact on our conclusions is relatively small (< 10%) (Lakin et al., 2018; Lujan et al., 2016).

Despite similar atrial remodelling and AF vulnerability with swim training, the extrapolation of murine findings to human athletes requires caution for several reasons. For example, our training protocol is not voluntary, although mice swam in thermoneutral tanks with water currents against which they naturally swim. The nocturnal mice also exercised during their sleeping periods, yet we previously showed our swim model does not elicit typical stress responses (Aschar-Sobbi et al., 2015). Moreover, mice gradually increase their level of engagement with the water current as the training program progresses, as indicated by increased O_2 consumption, which supports the conclusion that the mice tend to embrace the swimming exercise. It is also interesting that the intensity of the swim exercise in mice is substantially greater than when mice voluntarily run using free wheels (5534 ± 448 mL O_2 kg^{-1} h^{-1}, ∼2–2.5 METs) (Lakin et al., 2018), suggesting that swimming exercise in mice perhaps more closely mimics endurance exercise in humans. It will be interesting to compare the impact of voluntary running *vs.* swimming on cardiac remodelling and AF vulnerability, which are ongoing studies in our laboratory.

Alhough we observed striking parallels between the ability of increased MET-h $week^{-1}$ to promote AF vulnerability in swimming mice *vs.* human athletes, swimming mice require only 4–5 METs (above sleep levels), which contrasts with the much higher levels generally seen with endurance sport (i.e. >10 METs for cross-country skiing or >15 METs with running) (Jetté et al., 1990). Clearly, humans have a far greater capacity for increasing their $\dot{V}_{O_2}$ than mice. These differences in the relative changes in $\dot{V}_{O_2}$ between mice and endurance athletes during exercise are associated with corresponding huge disparities in HR increases to intense exercise (i.e. 4-fold in humans *vs.* 1.5-fold in mice) (Aschar-Sobbi et al., 2015). On the other hand, the elevations in venous filling pressure during exercise (to increase stroke volume via the Frank–Starling mechanism) are comparable between humans *vs.* mice (∼20–40 mmHg) (Aschar-Sobbi et al., 2015; Reeves et al., 1990). These observations suggest that the limited capacity for mice to increase their O_2 consumption (i.e. perform work) during exercise might

reflect their relative inability to increase cardiac output compared to humans. However, mice have much higher metabolic rates and their resting $\dot{V}_{O_2}$ during sleep (2303 ± 157 mL O_2 kg^{-1} h^{-1}) is ∼10-fold greater than humans at rest (1 MET, 210 mL O_2 kg^{-1} h^{-1}) (Jetté et al., 1990). Consequently, the final absolute $\dot{V}_{O_2}$ levels during swimming in mice still well exceeds that observed during exercise in humans engaged in endurance sport (Jones et al., 2021; Sousa et al., 2014).

Returning to the question of the J-shaped dependence of AF on exercise, it is interesting to point out that we saw no evidence of AF inducibility in our sedentary mice (Buckley et al., 2020), inconsistent with the J-shaped relationship observed in humans. However, our 'sedentary' mice show high levels of ambulatory activity and basal O_2 consumption (3117 ± 254 mL O_2 kg^{-1} h^{-1}, ∼1.3 METs) and are not generally obese (Lakin et al., 2018), whereas sedentary humans typically associated with increased AF risk tend to be obese and diabetic individuals (Al-Kaisey & Kalman, 2021; Bohne et al., 2019).

Caution should also be applied when comparing the results of the one-way ANOVA with Tukey's multiple comparisons tests and the linear regression analyses. We included both because they provide insightful information regarding the relationship of daily exercise dose with each investigated parameter yet demonstrate slightly varying interpretations of the data.

Summary and future directions

Our findings establish that increasing daily swim-exercise duration in mice dose-dependently promotes physiological ventricular remodelling at the same time as causing adverse atrial changes and cardiac autonomic nerve adaptations that can heighten AF vulnerability. Our findings support directly the previous human studies suggesting that CV health outcomes and AF vulnerability shows a J-shaped dependence on physical activity. We propose that the escalation of adverse atrial-specific changes as daily exercise dose increases is linked to progressive elevations in filling pressures, which is a common feature in most AF patients. This suggestion is consistent with our previous studies showing that the mechanosensitive cytokine TNF is required for exercise-induced adverse atrial remodelling (i.e. fibrosis, increased inflammatory cells and hypertrophy), as well as increased AF vulnerability in mice (Aschar-Sobbi et al., 2015; Lakin et al., 2019, 2023). Given this dependence of AF on TNF, we consider that future studies are needed to elucidate the direct involvement of the immune system and immune cells in the response of the atria to exercise, particularly because recent studies have suggested that macrophages can act as mechanosensors (Wong et al., 2021). Additionally, our mice were limited to male mice and it will be of interest to explore whether female mice respond similarly to exercise, given that female athletes are reportedly less vulnerable to AF (Svedberg et al., 2019). Because our studies were performed on mice during their light phase and because circadian rhythms are paramount in cardiovascular health, it will be of considerable interest to repeat our studies when mice exercise during their dark (awake) phase.

References

Aizer, A., Gaziano, J. M., Cook, N. R., Manson, J. E., Buring, J. E., & Albert, C. M. (2009). Relation of vigorous exercise to risk of atrial fibrillation. *American Journal of Cardiology*, **103**(11), 1572–1577.

Al-Kaisey, A. M., & Kalman, J. M. (2021). Obesity and atrial fibrillation: Epidemiology, pathogenesis and effect of weight loss. *Arrhythmia & Electrophysiology Review*, **10**(3), 159–164.

Amann, M., & Calbet, J. A. L. (2008). Convective oxygen transport and fatigue. *Journal of Applied Physiology*, **104**(3), 861–870.

Andersen, K., Farahmand, B., Ahlbom, A., Held, C., Ljunghall, S., Michaëlsson, K., & Sundström, J. (2013). Risk of arrhythmias in 52 755 long-distance cross-country skiers: A cohort study. *European Heart Journal*, **34**(47), 3624–3631.

Aschar-Sobbi, R., Izaddoustdar, F., Korogyi, A. S., Wang, Q., Farman, G. P., Yang, F., Yang, W., Dorian, D., Simpson, J. A., Tuomi, J. M., Jones, D. L., Nanthakumar, K., Cox, B., Wehrens, X. H. T., Dorian, P., & Backx, P. H. (2015). Increased atrial arrhythmia susceptibility induced by intense endurance exercise in mice requires TNFα. *Nature Communications*, **6**, 6018.

Barazi, N., Polidovitch, N., Debi, R., Yakobov, S., Lakin, R., & Backx, P. H. (2021). Dissecting the roles of the autonomic nervous system and physical activity on circadian heart rate fluctuations in mice. *Frontiers in Physiology*, **12**, 692247.

Benito, B., Gay-Jordi, G., Serrano-Mollar, A., Guasch, E., Shi, Y., Tardif, J.-C., Brugada, J., Nattel, S., & Mont, L. (2011). Cardiac arrhythmogenic remodeling in a rat model of long-term intensive exercise training. *Circulation*, **123**(1), 13–22.

Bizhanov, K. A., Abzaliyev, K. B., Baimbetov, A. K., Sarsenbayeva, A. B., & Lyan, E. (2023). Atrial fibrillation: Epidemiology, pathophysiology, and clinical complications (literature review). *Journal of Cardiovascular Electrophysiology*, **34**(1), 153–165.

Bohne, L. J., Johnson, D., Rose, R. A., Wilton, S. B., & Gillis, A. M. (2019). The association between diabetes mellitus and atrial fibrillation: Clinical and mechanistic insights. *Frontiers in Physiology*, **10**, 135.

Borresen, J., & Lambert, M. I. (2008). Autonomic control of heart rate during and after exercise. *Sports Medicine*, **38**(8), 633–646.

Buckley, B. J. R., Lip, G. Y. H., & Thijssen, D. H. J. (2020). The counterintuitive role of exercise in the prevention and cause of atrial fibrillation. *American Journal of Physiology. Heart and Circulatory Physiology*, **319**(5), H1051–H1058.

Carbone, S., Del Buono, M. G., Ozemek, C., & Lavie, C. J. (2019). Obesity, risk of diabetes and role of physical activity, exercise training and cardiorespiratory fitness. *Progress in Cardiovascular Diseases*, **62**(4), 327–333.

Claessen, G., Schnell, F., Bogaert, J., Claeys, M., Pattyn, N., De Buck, F., Dymarkowski, S., Claus, P., Carré, F., Van Cleemput, J., La Gerche, A., & Heidbuchel, H. (2018). Exercise cardiac magnetic resonance to differentiate athlete's heart from structural heart disease. *European Heart Journal - Cardiovascular Imaging*, **19**(9), 1062–1070.

Conti, V., Migliorini, F., Pilone, M., Barriopedro, M. I., Ramos-Álvarez, J. J., Montero, F. J. C., & Maffulli, N. (2021). Right heart exercise-training-adaptation and remodelling in endurance athletes. *Scientific Reports*, **11**(1), 22532.

De Jong, A. M., Maass, A. H., Oberdorf-Maass, S. U., Van Veldhuisen, D. J., Van Gilst, W. H., & Van Gelder, I. C. (2011). Mechanisms of atrial structural changes caused by stretch occurring before and during early atrial fibrillation. *Cardiovascular Research*, **89**(4), 754–765.

D'Souza, A., Bucchi, A., Johnsen, A. B., Logantha, S. J. R. J., Monfredi, O., Yanni, J., Prehar, S., Hart, G., Cartwright, E., Wisloff, U., Dobryznski, H., DiFrancesco, D., Morris, G. M., & Boyett, M. R. (2014). Exercise training reduces resting heart rate via downregulation of the funny channel HCN4. *Nature Communications*, **5**(1).

Dumke, C. L., Mark Davis, J., Angela Murphy, E., Nieman, D. C., Carmichael, M. D., Quindry, J. C., Travis Triplett, N., Utter, A. C., Gross Gowin, S. J., Henson, D. A., McAnulty, S. R., & McAnulty, L. S. (2009). Successive bouts of cycling stimulates genes associated with mitochondrial biogenesis. *European Journal of Applied Physiology*, **107**(4), 419–427.

Dzeshka, M. S., Lip, G. Y. H., Snezhitskiy, V., & Shantsila, E. (2015). Cardiac fibrosis in patients with atrial fibrillation. *Journal of the American College of Cardiology*, **66**(8), 943–959.

Elliott, A. D., Linz, D., Verdicchio, C. V., & Sanders, P. (2018). Exercise and atrial fibrillation: Prevention or causation? *Heart, Lung and Circulation*, **27**(9), 1078–1085.

Elosua, R., Arquer, A., Mont, L., Sambola, A., Molina, L., García-Morán, E., Brugada, J., & Marrugat, J. (2006). Sport practice and the risk of lone atrial fibrillation: A case–control study. *International Journal of Cardiology*, **108**(3), 332–337.

Engelmann, M. D. M., & Svendsen, J. H. (2005). Inflammation in the genesis and perpetuation of atrial fibrillation. *European Heart Journal*, **26**(20), 2083–2092.

Estes, N. A. M., & Madias, C. (2017). Atrial fibrillation in athletes. *JACC: Clinical Electrophysiology*, **3**(9), 921–928.

Fiuza-Luces, C., Santos-Lozano, A., Joyner, M., Carrera-Bastos, P., Picazo, O., Zugaza, J. L., Izquierdo, M., Ruilope, L. M., & Lucia, A. (2018). Exercise benefits in cardiovascular disease: Beyond attenuation of traditional risk factors. *Nature Reviews Cardiology*, **15**(12), 731–743.

Franklin, B. A., Thompson, P. D., Al-Zaiti, S. S., Albert, C. M., Hivert, M.-F., Levine, B. D., Lobelo, F., Madan, K., Sharrief, A. Z., & Eijsvogels, T. M. H. (2020). Exercise-related acute cardiovascular events and potential deleterious adaptations following long-term exercise training: Placing the risks into perspective–an update: A scientific statement from the american heart association. *Circulation*, **141**(13), e705–e736.

Gerche, A. L., & Schmied, C. M. (2013). Atrial fibrillation in athletes and the interplay between exercise and health. *European Heart Journal*, **34**(47), 3599–3602.

Goldsmith, R. L., Bloomfield, D. M., & Rosenwinkel, E. T. (2000). Exercise and autonomic function. *Coronary Artery Disease*, **11**(2), 129–135.

Gourine, A. V., & Ackland, G. L. (2019). Cardiac vagus and exercise. *Physiology*, **34**(1), 71–80.

Grundy, D. (2015). Principles and standards for reporting animal experiments in *The Journal of Physiology* and *Experimental Physiology*. *The Journal of Physiology*, **593**(12), 2547–2549.

Guasch, E., Mont, L., & Sitges, M. (2018). Mechanisms of atrial fibrillation in athletes: What we know and what we do not know. *Netherlands Heart Journal*, **26**(3), 133–145.

Hadi, A. M., Mouchaers, K. T. B., Schalij, I., Grunberg, K., Meijer, G. A., Vonk-Noordegraaf, A., van der Laarse, W. J., & Beliën, J. A. M. (2011). Rapid quantification of myocardial fibrosis: A new macro-based automated analysis. *Cellular Oncology*, **34**(4), 343–354.

Hamilton, D. R., Dani, R. S., Semlacher, R. A., Smith, E. R., Kieser, T. M., & Tyberg, J. V. (1994). Right atrial and right ventricular transmural pressures in dogs and humans. Effects of the pericardium. *Circulation*, **90**(5), 2492–2500.

Holloszy, J. O., & Coyle, E. F. (1984). Adaptations of skeletal muscle to endurance exercise and their metabolic consequences. *Journal of Applied Physiology*, **56**(4), 831–838.

Hulsmans, M., Schloss, M. J., Lee, I. H., Bapat, A., Iwamoto, Y., Vinegoni, C., Paccalet, A., Yamazoe, M., Grune, J., Pabel, S., Momin, N., Seung, H., Kumowski, N., Pulous, F. E., Keller, D., Bening, C., Green, U., Lennerz, J. K., Mitchell, R. N., … Nahrendorf, M. (2023). Recruited macrophages elicit atrial fibrillation. *Science (80-)*, **381**(6654), 231–239.

Ishii, K., Kuwahara, M., Tsubone, H., & Sugano, S. (1996). Autonomic nervous function in mice and voles (Microtus arvalis): Investigation by power spectral analysis of heart rate variability. *Laboratory Animals*, **30**(4), 359–364.

Jalife, J., & Kaur, K. (2015). Atrial remodeling, fibrosis, and atrial fibrillation. *Trends in Cardiovascular Medicine*, **25**(6), 475–484.

Janssen, B. J. A., De Celle, T., Debets, J. J. M., Brouns, A. E., Callahan, M. F., & Smith, T. L. (2004). Effects of anesthetics on systemic hemodynamics in mice. *American Journal of Physiology. Heart and Circulatory Physiology*, **287**(4), H1618–H1624.

Jetté, M., Sidney, K., & Blümchen, G. (1990). Metabolic equivalents (METS) in exercise testing, exercise prescription, and evaluation of functional capacity. *Clinical Cardiology*, **13**(8), 555–565.

Jones, A. M., Kirby, B. S., Clark, I. E., Rice, H. M., Fulkerson, E., Wylie, L. J., Wilkerson, D. P., Vanhatalo, A., & Wilkins, B. W. (2021). Physiological demands of running at 2-hour marathon race pace. *Journal of Applied Physiology*, **130**(2), 369–379.

Joyner, M. J., & Casey, D. P. (2015). Regulation of increased blood flow (Hyperemia) to muscles during exercise: A hierarchy of competing physiological needs. *Physiological Reviews*, **95**(2), 549–601.

Kontro, T. K., Sarna, S., Kaprio, J., & Kujala, U. M. (2018). Mortality and health-related habits in 900 Finnish former elite athletes and their brothers. *British Journal of Sports Medicine*, **52**(2), 89–95.

Król, W., Jędrzejewska, I., Konopka, M., Burkhard-Jagodzińska, K., Klusiewicz, A., Pokrywka, A., Chwalbińska, J., Sitkowski, D., Dłużniewski, M., Mamcarz, A., & Braksator, W. (2016). Left atrial enlargement in young high-level endurance athletes – Another sign of athlete's heart? *Journal of Human Kinetics*, **53**, 81–90.

Lakin, R., Debi, R., Yang, S., Polidovitch, N., Goodman, J. M., & Backx, P. H. (2021). Differential negative effects of acute exhaustive swim exercise on the right ventricle are associated with disproportionate hemodynamic loading. *American Journal of Physiology. Heart and Circulatory Physiology*, **320**(4), H1261–H1275.

Lakin, R., Guzman, C., Izaddoustdar, F., Polidovitch, N., Goodman, J. M., & Backx, P. H. (2018). Changes in heart rate and its regulation by the autonomic nervous system do not differ between forced and voluntary exercise in mice. *Frontiers in Physiology*, **9**, 841.

Lakin, R., Polidovitch, N., Yang, S., Guzman, C., Gao, X., Wauchop, M., Burns, J., Izaddoustdar, F., & Backx, P. H. (2019). Inhibition of soluble TNFα prevents adverse atrial remodeling and atrial arrhythmia susceptibility induced in mice by endurance exercise. *Journal of Molecular and Cellular Cardiology*, **129**, 165–173.

Lakin, R., Polidovitch, N., Yang, S., Parikh, M., Liu, X., Debi, R., Gao, X., Chen, W., Guzman, C., Yakobov, S., Izaddoustdar, F., Wauchop, M., Lei, Q., Xu, W., Nedospasov, S. A., Christoffels, V. M., & Backx, P. H. (2023). Cardiomyocyte and endothelial cells play distinct roles in the tumor necrosis factor (TNF)-dependent atrial responses and increased atrial fibrillation vulnerability induced by endurance exercise training in mice. *Cardiovascular Research*, **119**(16), 2607–2622.

Lee, D., Pate, R. R., Lavie, C. J., Sui, X., Church, T. S., & Blair, S. N. (2014). Leisure-time running reduces all-cause and cardiovascular mortality risk. *Journal of the American College of Cardiology*, **64**(5), 472–481.

Li, S., Zhang, Z., Scherlag, B. J., & Po, S. S. (2010). Atrial fibrillation in athletes - the story behind the running hearts. *Journal of Atrial Fibrillation*, **2**(5), 231.

Lujan, H. L., Rivers, J. P., & DiCarlo, S. E. (2016). Complex and interacting influences of the autonomic nervous system on cardiac electrophysiology in conscious mice. *Autonomic Neuroscience*, **201**, 24–31.

Mai, H., Luo, J., Hoeher, L., Al-Maskari, R., Horvath, I., Chen, Y., Kofler, F., Piraud, M., Paetzold, J. C., Modamio, J., Todorov, M., Elsner, M., Hellal, F., & Ertürk, A. (2024). Whole-body cellular mapping in mouse using standard IgG antibodies. *Nature Biotechnology*, Advance online publication. https://doi.org/10.1038/s41587-023-01846-0.

Małek, Ł. A., & Bucciarelli-Ducci, C. (2020). Myocardial fibrosis in athletes—Current perspective. *Clinical Cardiology*, **43**(8), 882–888.

McEvoy, G. (2012). *Drug Information 2012*. American Society of Health-System Pharmacists.

McNamara, D. A., Aiad, N., Howden, E., Hieda, M., Link, M. S., Palmer, D., Samels, M., Everding, B., Ng, J., Adams-Huet, B., Opondo, M., Sarma, S., & Levine, B. D. (2019). Left atrial electromechanical remodeling following 2 years of high-intensity exercise training in sedentary middle-aged adults. *Circulation*, **139**(12), 1507–1516.

Mier, C. M., Turner, M. J., Ehsani, A. A., & Spina, R. J. (1997). Cardiovascular adaptations to 10 days of cycle exercise. *Journal of Applied Physiology*, **83**(6), 1900–1906.

Miragoli, M., & Glukhov, A. V.(2015). Atrial fibrillation and fibrosis: Beyond the cardiomyocyte centric view. *BioMed ReSearch International*, **2015**, 798768.

Mittleman, M. A., Maclure, M., Tofler, G. H., Sherwood, J. B., Goldberg, R. J., & Muller, J. E. (1993). Triggering of acute myocardial infarction by heavy physical exertion – protection against triggering by regular exertion. *New England Journal of Medicine*, **329**(23), 1677–1683.

Mont, L. (2002). Long-lasting sport practice and lone atrial fibrillation. *European Heart Journal*, **23**(6), 477–482.

Mont, L., Tamborero, D., Elosua, R., Molina, I., Coll-Vinent, B., Sitges, M., Vidal, B., Scalise, A., Tejeira, A., Berruezo, A., & Brugada, J. (2008). Physical activity, height, and left atrial size are independent risk factors for lone atrial fibrillation in middle-aged healthy individuals. *European Pharmacopoeia*, **10**(1), 15–20.

Morganroth, J. (1975). Comparative left ventricular dimensions in trained athletes. *Annals of Internal Medicine*, **82**(4), 521–524.

Neuberger, H.-R., Schotten, U., Blaauw, Y., Vollmann, D., Eijsbouts, S., van Hunnik, A., & Allessie, M. (2006). Chronic atrial dilation, electrical remodeling, and atrial fibrillation in the goat. *Journal of the American College of Cardiology*, **47**(3), 644–653.

Nguyen, T.-N., Siddiqui, G., Veldhuis, N. A., & Poole, D. P. (2022). Diverse roles of TRPV4 in macrophages: A need for unbiased profiling. *Frontiers in Immunology*, **12**, 828115.

Pathak, R. K., Elliott, A., Middeldorp, M. E., Meredith, M., Mehta, A. B., Mahajan, R., Hendriks, J. M. L., Twomey, D., Kalman, J. M., Abhayaratna, W. P., Lau, D. H., & Sanders, P. (2015). Impact of CARDIOrespiratory FITness on arrhythmia recurrence in obese individuals with atrial fibrillation. *Journal of the American College of Cardiology*, **66**(9), 985–996.

Peritz, D. C., Catino, A. B., Csecs, I., Kaur, G., Kheirkhahan, M., Loveless, B., Wasmund, S., Kholmovski, E., Morris, A., & Marrouche, N. F. (2020). High-intensity endurance training is associated with left atrial fibrosis. *American Heart Journal*, **226**, 206–213.

Rahmutula, D., Zhang, H., Wilson, E. E., & Olgin, J. E. (2019). Absence of natriuretic peptide clearance receptor attenuates TGF-β1-induced selective atrial fibrosis and atrial fibrillation. *Cardiovascular Research*, **115**(2), 357–372.

Rebecchi, M., Panattoni, G., Edoardo, B., Ruvo, E., Sciarra, L., Politano, A., Sgueglia, M., Ricagni, C., Verbena, S., Crescenzi, C., Sangiorgi, C., Borrelli, A., De Luca, L., Scarà, A., Grieco, D., Jacomelli, I., Martino, A., & Calò L. (2021). Atrial fibrillation and autonomic nervous system: A translational approach to guide therapeutic goals. *Journal of Arrhythmia*, **37**(2), 320–330.

Reeves, J. T., Groves, B. M., Cymerman, A., Sutton, J. R., Wagner, P. D., Turkevich, D., & Houston, C. S. (1990). Operation Everest II: Cardiac filling pressures during cycle exercise at sea level. *Respiration Physiology*, **80**(2–3), 147–154.

Rezende, L. F. M. d., Sá, T. H. d., Markozannes, G., Rey-López, J. P., Lee, I.-M., Tsilidis, K. K., Ioannidis, J. P. A., & Eluf-Neto, J. (2018). Physical activity and cancer: An umbrella review of the literature including 22 major anatomical sites and 770 000 cancer cases. *British Journal of Sports Medicine*, **52**(13), 826–833.

Sharma, S., Merghani, A., & Mont, L. (2015). Exercise and the heart: The good, the bad, and the ugly. *European Heart Journal*, **36**(23), 1445–1453.

Singh, R., Pattisapu, A., & Emery, M. S. (2020). US physical activity guidelines: Current state, impact and future directions. *Trends in Cardiovascular Medicine*, **30**(7), 407–412.

Sohns, C., & Marrouche, N. F. (2020). Atrial fibrillation and cardiac fibrosis. *European Heart Journal*, **41**(10), 1123–1131.

Sousa, A. C., Vilas-Boas, J. P., & Fernandes, R. J. (2014). VO2 kinetics and metabolic contributions whilst swimming at 95, 100, and 105% of the velocity at VO2max. *BioMed Research International*, **2014**, 675363.

Speakman, J. R. (2013). Measuring energy metabolism in the mouse – Theoretical, practical, and analytical considerations. *Frontiers in Physiology*, **4**, 34.

Svedberg, N., Sundström, J., James, S., Hållmarker, U., Hambraeus, K., & Andersen, K. (2019). Long-term incidence of atrial fibrillation and stroke among cross-country skiers: Cohort study of endurance-trained male and female athletes. *Circulation*, **140**(11), 910–920.

Swain, D. P. (2005). Moderate or vigorous intensity exercise: Which is better for improving aerobic fitness? *Preventive Cardiology*, **8**(1), 55–58.

Swanson, D. R. (2006). Atrial fibrillation in athletes: Implicit literature-based connections suggest that overtraining and subsequent inflammation may be a contributory mechanism. *Medical Hypotheses*, **66**(6), 1085–1092.

Tamaki, S., Mano, T., Sakata, Y., Ohtani, T., Takeda, Y., Kamimura, D., Omori, Y., Tsukamoto, Y., Ikeya, Y., Kawai, M., Kumanogoh, A., Hagihara, K., Ishii, R., Higashimori, M., Kaneko, M., Hasuwa, H., Miwa, T., Yamamoto, K., & Komuro, I. (2013). Interleukin-16 promotes cardiac fibrosis and myocardial stiffening in heart failure with preserved ejection fraction. *PLoS ONE*, **8**(7), e68893.

Turagam, M. K., Flaker, G. C., Velagapudi, P., Vadali, S., & Alpert, M. A. (2015). Atrial fibrillation in athletes: Pathophysiology, clinical presentation, evaluation and management. *Journal of Atrial Fibrillation*, **8**(4), 1309.

Uechi, M., Asai, K., Osaka, M., Smith, A., Sato, N., Wagner, T. E., Ishikawa, Y., Hayakawa, H., Vatner, D. E., Shannon, R. P., Homcy, C. J., & Vatner, S. F. (1998). Depressed heart rate variability and arterial baroreflex in conscious transgenic mice with overexpression of cardiac $G_{s\alpha}$. *Circulation Research*, **82**(4), 416–423.

Vranka, I., Penz, P., & Dukát, A. (2007). Atrial conduction delay and its association with left atrial dimension, left atrial pressure and left ventricular diastolic dysfunction in patients at risk of atrial fibrillation. *Experimental & Clinical Cardiology*, **12**(4), 197–201.

Wong, N. R., Mohan, J., Kopecky, B. J., Guo, S., Du, L., Leid, J., Feng, G., Lokshina, I., Dmytrenko, O., Luehmann, H., Bajpai, G., Ewald, L., Bell, L., Patel, N., Bredemeyer, A., Weinheimer, C. J., Nigro, J. M., Kovacs, A., Morimoto, S., … Lavine, K. J. (2021). Resident cardiac macrophages mediate adaptive myocardial remodeling. *Immunity*, **54**(9), 2072–2088.e7.

Yamashita, T., Murakawa, Y., Sezaki, K., Inoue, M., Hayami, N., Shuzui, Y., & Omata, M. (1997). Circadian variation of paroxysmal atrial fibrillation. *Circulation*, **96**(5), 1537–1541.

Yamashita, T., Sekiguchi, A., Iwasaki, Y., Date, T., Sagara, K., Tanabe, H., Suma, H., Sawada, H., & Aizawa, T. (2010). Recruitment of immune cells across atrial endocardium in human atrial fibrillation. *Circulation Journal*, **74**(2), 262–270.

Yeh, Y.-H., Lemola, K., & Nattel, S.(2007). Vagal atrial fibrillation. *Acta Cardiological Sinica*, **23**(1), 1–12.

Additional information

Data availability statement

Additional data underlying this article will be shared upon reasonable request to the corresponding authors.

Competing interests

The authors declare that they have no competing interests.

Author contributions

Experiments were performed at York University, Department of Biology. R.A.G., S.Y., R.L. and P.H.B. were responsible for the conception and design, acquisition, analysis and interpretation of data for the work, as well as drafting the work and revising it critically for important intellectual content. N.P., R.D., V.C.S. and D.A.H. were responsible for a part of the acquisition and analysis and drafting the work. All authors approved the final version of this manuscript submitted for publication. All authors agree to be accountable for all aspects of the work.

Funding

P.H.B. acknowledges project grants from the Canadian Institutes of Health Research (CIHR) [MOP-119339 and MOP 125950], a Canada Research Chair in Cardiovascular Biology from the CIHR, and a John Evans Leader Award for equipment from the Canadian Foundation for Innovation. CIHR also provided a Postdoctoral Fellowship to R.L. D.A.H. acknowledges a project grant from the Natural Sciences and Engineering Research

Council of Canada [MOP-38462] and a Canadian Research Chair in Cell Physiology from the NSERC.

Acknowledgements

We thank all the volunteers who assisted in helping swim the mice for this study.

Keywords

atrial fibrillation, atrial remodelling, cardiovascular, daily exercise duration, exercise dose

Supporting information

Additional supporting information can be found online in the Supporting Information section at the end of the HTML view of the article. Supporting information files available:

Peer Review History
Supplemental information